1 **Title:** Mitochondrial-Encoded Peptide MOTS-c is an Exercise-Induced Regulator of Aging
2 Metabolic Homeostasis and Physical Capacity

3

4

5 **Authors:** Joseph C. Reynolds[1], Rochelle W. Lai[1], Jonathan S.T. Woodhead[5,6], James H. Joly[4],
6 Cameron J. Mitchell[7,9], David Cameron-Smith[7], Ryan Lu[1], Pinchas Cohen[1,2], Nicholas A.
7 Graham[2,4], Bérénice A. Benayoun[1,2,3], Troy L. Merry[5,6], Changhan Lee[1,2,8]*.

8

9 [1] Leonard Davis School of Gerontology, University of Southern California, Los Angeles, CA
10 90089.
11 [2] USC Norris Comprehensive Cancer Center, Los Angeles, CA 90089.
12 [3] USC Stem Cell Initiative, Los Angeles, CA 90089.
13 [4] USC Mork Family Department of Chemical Engineering and Materials Science, Los Angeles,
14 CA 90089.
15 [5] Discipline of Nutrition, Faculty of Medical and Health Sciences, The University of Auckland,
16 Auckland, New Zealand
17 [6] Maurice Wilkins Centre for Molecular Biodiscovery, The University of Auckland, Auckland,
18 New Zealand
19 [7] Liggins Institute, The University of Auckland, Auckland, New Zealand
20 [8] Biomedical Science, Graduate School, Ajou University, Suwon 16499, Korea.
21 [9] School of Kinesiology, University of British Colombia, Vancouver, BC, Canada V6T 1Z3

22

23 *corresponding author: changhan.lee@usc.edu

24

25

26

27

28

29

**Abstract:**

Healthy aging can be promoted by enhancing metabolic fitness and physical capacity (*1, 2*). Mitochondria are chief metabolic organelles with strong implications in aging (*3-8*). In addition to their prominent role in bioenergetics, mitochondria also coordinate broad physiological functions by communicating to other cellular compartments or distal cells using multiple factors (*9, 10*), including peptides that are encoded within their own independent genome (*11, 12*). However, it is unknown if aging is actively regulated by factors encoded in the mitochondrial genome. MOTS-c is a mitochondrial-encoded peptide that regulates metabolic homeostasis (*13, 14*), in part, by translocating to the nucleus to regulate adaptive nuclear gene expression in response to cellular stress (*15-17*). Here, we report that MOTS-c is an exercise-induced mitochondrial-encoded peptide that significantly enhanced physical performance when administered to young (2 mo.), middle-aged (12 mo.), and old (22 mo.) mice. In humans, we found that endogenous MOTS-c levels significantly increased in response to exercise in skeletal muscle (11.9-fold) and in circulation (1.5-fold). Systemic MOTS-c treatment in mice significantly enhanced the performance on a treadmill of all age groups (~2-fold). MOTS-c regulated (i) nuclear genes, including those related to metabolism and protein homeostasis, (ii) glucose and amino acid metabolism in skeletal muscle, and (iii) myoblast adaptation to metabolic stress. Late-life (23.5 mo.) initiated intermittent MOTS-c treatment (3x/week) improved physical capacity and trended towards increasing lifespan. Our data indicate that aging is regulated by genes that are encoded not only in the nuclear genome (*18, 19*), but also in the mitochondrial genome. Considering that aging is the major risk factor for multiple chronic diseases (*20, 21*), our study provides new grounds for further investigation into mitochondrial-encoded regulators of healthy lifespan.

**Main Text:**

Organismal fitness requires continuous adaptive cellular stress responses to the ever-shifting internal and external environment. The capacity to maintain metabolic homeostasis declines with age, which impedes parenchymal function and ultimately diminishes physical capacity. Mitochondria not only produce the bulk of cellular energy, but also coordinate adaptive cellular homeostasis by dynamically communicating to the nucleus (*9*) and other subcellular compartments

60  (*22*). Mitochondrial communication is mediated by multiple nuclear-encoded proteins, transient

61  molecules, and mitochondrial metabolites (*23*).

62  Mitochondria possess a distinct circular genome that has been traditionally known to host only 13

63  protein-coding genes. However, short open reading frames (sORFs) encoded in the mitochondrial

64  genome have been recently identified. Such sORFs produce bioactive peptides, collectively

65  referred to as mitochondrial-derived peptides (MDPs), with broad physiological functions (*11, 12*).

66  MOTS-c (mitochondrial ORF of the 12S rDNA type-c) is an MDP that promotes metabolic

67  homeostasis, in part, via AMPK (*13, 14*) and by directly regulating adaptive nuclear gene

68  expression following nuclear translocation (*15, 16*). MOTS-c expression is age-dependent and

69  detected in multiple tissues, including skeletal muscle, and in circulation (*13, 14, 24*), thus it has

70  been dubbed a "mitochondrial hormone" (*14*) or "mitokine" (*25, 26*). In fact, systemic MOTS-c

71  treatment reversed diet-induced obesity and diet- and age-dependent insulin resistance in mice

72  (*13*). We tested if MOTS-c functions as a mitochondrial-encoded regulator of physical capacity

73  and performance (*2, 27, 28*) in young (2 mo.), middle-aged (12 mo.), and old (22 mo.) mice.

74  To determine if endogenous MOTS-c responds to physical exertion, and thus may be involved in

75  driving adaptation to enhance physical capacity, we collected skeletal muscle and plasma from

76  sedentary healthy young male volunteers (24.5 ± 3.7 years old and BMI 24.1 ± 2.1) that exercised

77  on a stationary bicycle (Fig. 1A). Samples were collected before, during (plasma only), and after

78  exercise and following a 4-hour rest. Western blotting revealed that endogenous MOTS-c levels

79  in skeletal muscle significantly increased after exercise (11.9-fold) and remained elevated after a

80  4-hour rest (18.9-fold) (Fig. 1B, C). ELISA revealed that circulating endogenous MOTS-c levels

81  also significantly increased during (1.6-fold) and after (1.5-fold) exercise, which then returned to

82  baseline after 4 hours of resting (Fig. 1D, fig. S1). These findings suggest that exercise induces the

83  expression of mitochondrial-encoded regulatory peptides in humans.

84  We next probed if MOTS-c functions as an exercise-induced mitochondrial signal that improves

85  physical capacity by treating young mice (CD-1; outbred) daily with MOTS-c [5mg/kg/day;

86  intraperitoneal injections (IP)] for 2 weeks. The rotarod performance test, whereby mice are placed

87  on a rotating rod, revealed that daily MOTS-c significantly improved physical capacity (fig. S2A),

88  but not grip strength (fig. S2B) in young mice. Because the rotarod test can also be affected by

89 cognitive capacity, we assessed learning and memory using the Barnes maze and found no
90 improvement (fig. S2C, D).

91 A treadmill running test confirmed that MOTS-c treatment can enhance physical performance.
92 Because MOTS-c is regulator of metabolic homeostasis that prevented high-fat diet (HFD)-
93 induced obesity and insulin resistance (*13*), we tested if MOTS-c also improved running
94 performance under metabolic (dietary) stress. We fed young mice (CD-1) a HFD (60% calories
95 from fat) and treated them with 2 doses of MOTS-c (5 and 15 mg/kg/day; IP) (fig. S3A). Mice on
96 the higher dose of MOTS-c showed significantly superior running capacity following 10 days of
97 treatment (Fig. 2A-C), but not 7 days of treatment (fig. S4A). We progressively increased the
98 treadmill speed to test both endurance and speed. The final stage, which required mice to sprint
99 (23m/s), was reached by 100% of mice on the higher dose of MOTS-c, but only 16.6% in the lower
100 dose and control (vehicle) groups (Fig. 2D). Body composition analysis using a time-domain NMR
101 analyzer revealed that both doses of MOTS-c significantly retarded fat gain and that the high dose
102 significantly increased lean mass in young mice (CD-1) (fig. S5A-C), in accord with prior reports
103 (*13*).

104 In young CD-1 mice, we simultaneously initiated MOTS-c treatment and a HFD (fig. S3A). To
105 test if MOTS-c can improve physical performance in mice that have been on a HFD, we fed young
106 C57BL/6J mice a HFD, or a normal diet, for 2 weeks before initiating daily MOTS-c injections
107 (15 mg/kg/day) for 2 weeks prior to a treadmill running test (fig. S3B). MOTS-c treatment
108 significantly enhanced running performance on the treadmill regardless of the diet (Fig. 2E-G, fig.
109 S4B). MOTS-c treatment enabled 25% of the young C57BL/6J mice to enter the final running
110 stage (highest speed) on a normal diet, but none on a HFD (Fig. 2H). Consistent with our prior
111 study (*13*), MOTS-c treatment curbed HFD-induced weight gain in C57BL/6J mice (fig. S5D),
112 which was largely driven by reduced fat accumulation (fig. S5E), but not loss of lean mass (fig.
113 S5F), as determined by an NMR-based body composition analysis. Further, targeted metabolomics
114 revealed that MOTS-c treatment significantly regulated (i) glycolysis/PPP (pentose phosphate
115 pathway) and (ii) amino acid metabolism (Fig. 2I, fig. S3B) in skeletal muscle, but not in liver,
116 consistent with our previous study (*13*). Together, these data indicate that MOTS-c treatment can
117 improve overall physical performance, in part, by targeting skeletal muscle metabolism in young
118 mice.

119      Aging is accompanied by a progressive decline in mitochondrial function (*1, 8*) and loss of

120      metabolic homeostasis, in which MOTS-c may play a role (*2, 9*). Aging is associated with reduced

121      MOTS-c levels in certain tissues, including the skeletal muscle, and in circulation (*13, 24*). We

122      previously showed that an acute one-week MOTS-c treatment reversed age-dependent insulin

123      resistance in mouse skeletal muscle (*13*). Thus, we investigated if promoting metabolic

124      homeostasis by MOTS-c treatment could reverse age-dependent decline in physical capacity.

125      Middle-aged (12 mo.) and old (22 mo.) C57BL/6N mice were treated daily with MOTS-c (15

126      mg/kg/day; IP) for 2 weeks, then subjected to a treadmill running test (Fig. 3A). Both middle-aged

127      and old mice ran significantly longer following MOTS-c treatment (Fig. 3B). Old mice ran longer

128      (2-fold) (Fig. 3C) and farther (2.16-fold) (Fig. 3D) when treated with MOTS-c. Further, MOTS-c

129      enabled 17% of the old mice to enter the final running stage (highest speed), whereas none in the

130      untreated group were successful (Fig. 3E). Notably, MOTS-c treatment enabled old mice to

131      outperform untreated middle-aged mice, suggesting a more pervasive physical re-programming

132      rather than just rejuvenation. Respiratory exchange ratio (RER), measured using a metabolic cage,

133      indicates fuel preference (1.0: carbohydrates, 0.7: fat). "Metabolic flexibility", which refers to the

134      overall adaptive capacity to a shift in metabolic supply-demand equilibrium (*e.g.* exercise),

135      declines with age (*29, 30*). Indeed, old mice relied on carbohydrates regardless of the time of day

136      (Fig. 3F), whereas middle-aged mice, and MOTS-c-treated old mice, exhibited a circadian-

137      dependent shift in fuel usage that favored fat during the daytime (Fig. 3F), coinciding with the

138      low-feeding hours (fig. S6). Metabolomic analysis on skeletal muscle collected immediately post-

139      exercise (a 30-minute run at a fixed moderate speed) in MOTS-c-treated (2 weeks) mice revealed

140      that MOTS-c significantly regulated glycolysis and amino acid metabolism (Fig. 3G); the skeletal

141      muscles of non-exercised mice did not show significant alterations in response to MOTS-c (fig.

142      S7), suggesting that MOTS-c induces an adaptive metabolic response to exercise. To begin to

143      understand the molecular mechanisms underlying the effects of MOTS-c, we performed RNA-seq

144      analysis on the same skeletal muscles used for metabolomics. Although individual-to-individual

145      variability was high, Gene Set Enrichment Analysis (GSEA) using the KEGG pathway database

146      revealed that MOTS-c regulated processes related to (i) metabolism, including those known to be

147      regulated by MOTS-c (*e.g.* AMPK signaling, glycolysis, and central carbon metabolism) (*13, 15*),

148      and (ii) longevity (FDR < 15%; select pathways in Fig. 3H; full analysis in able S1). Gene

149      Ontology Biological Process (GO_BP) analysis revealed a broader range of processes, including

150    metabolism (lipid, carbohydrate, amino acid, and nucleotides), oxidative stress response, immune

151    response, and nuclear transport (FDR < 15%; select pathways in fig. S8; full analysis in table S2),

152    again, consistent with our previous studies (*13, 15*). The rotarod performance test confirmed that

153    MOTS-c treatment improved physical capacity in old mice (fig. S9A), while learning and memory

154    was not affected as determined using the Y-maze test (fig. S9B), consistent with our observations

155    in young mice (fig. S2). Together, these data suggest that MOTS-c treatment can significantly

156    improve physical capacity in old mice, in part, by regulating skeletal function and improving

157    "metabolic flexibility".

158    Age is the major risk factor for many chronic diseases and interventions that delay aging may

159    extend healthy lifespan (*20, 31-33*). Anti-aging interventions that are applied later in life would be

160    more translationally feasible compared to life-long treatments (*34, 35*). Building on the treadmill

161    running tests, we tested if a late-life initiated (~24 mo.) intermittent (LLII) MOTS-c treatment

162    (3x/week; 15mg/kg/day) would improve healthy lifespan (Fig. 3A). To assess healthspan, towards

163    the end-of-life (>30 mo.), we performed a battery of physical tests to further probe the effect of

164    MOTS-c on reversing age-dependent physical decline (Fig. 3A). LLII MOTS-c improved (i) grip

165    strength (Fig. 4A), (ii) gait, assessed by stride length (Fig. 4B), and (iii) physical performance,

166    assessed by a 60-second walking test (running was not possible at this age) (Fig. 4C). In humans,

167    reduced stride length and walking capacity are strongly linked to mortality and morbidity (*36*).

168    Together, these data indicate that LLII MOTS-c treatment improves physical capacity in old mice.

169    Independent lines of research have shown that MOTS-c is a mitochondrial-encoded metabolic

170    regulator at the cellular and organismal level (*13, 15, 24, 37-41*). We posited that LLII MOTS-c

171    treatment would cause metabolic reprogramming in old mice. Consistent with our previous report

172    (*13*), non-fasting blood glucose was better maintained in LLII MOTS-c-treated old mice (30 mo.;

173    Fig. 4D). Over course of their life, LLII MOTS-c-treated mice showed comparable body weight

174    to their untreated counterparts (Fig. 4E, F) However, total food intake was significantly reduced

175    (Fig. 4G, H, fig. S6), whereas total activity was significantly higher (fig. S10). Body composition

176    analysis using a time-domain NMR analyzer revealed significant reduction of fat mass (Fig. 4I, J)

177    and a modest increase in lean mass (Fig. 4K, L). The RER, measured using metabolic cages, at 30

178    mo. revealed increased fat utilization, consistent with that obtained at ~23.5 mo. (Fig. 3F), but with

179    a circadian shift (fig. S11); this is also consistent with reduced total fat mass (Fig. 4I, J, fig. S5B,

180   E) and increased lipid utilization (*13, 41*). Ultimately, LLII MOTS-c treatment showed a trend

181   towards increased median (6.4%) and maximum (7.0%) lifespan and reduced hazard ratio (0.654);

182   *P*=0.05 until 31.8 months (Fig. 4M). Larger cohorts will be needed to confirm the broader

183   significance of MOTS-c treatment on overall longevity. These data suggest that LLII MOTS-c

184   treatment improves overall physical capacity in old mice and may compress morbidity and increase

185   healthspan.

186   Skeletal muscle must adapt to various exercise-induced challenges (*42*), including nutrient (*e.g.*

187   metabolic supply-demand imbalance) (*43*), oxidative (*44, 45*), and heat stress (*42, 46*), which share

188   mitochondria as a common denominator. Because MOTS-c enhanced cellular resistance against

189   metabolic/oxidative stress (*15*), we tested if MOTS-c treatment improved skeletal muscle

190   adaptation to metabolic stress using C2C12 mouse myoblast cells. Using crystal violet staining to

191   determine cellular viability, we found that MOTS-c (10μM) treatment significantly protected

192   C2C12 cells (~2-fold) from 48 hours of metabolic stress [glucose restriction (GR; 0.5 g/L) and

193   serum deprivation (SD; 1% FBS)] (Fig. 5A). Next, we tested the replicative capacity of C2C12

194   cells following prolonged metabolic stress as a functional marker of protection. C2C12 cells were

195   metabolically stressed (GR/SD) for one week with daily MOTS-c (10μM) treatment, then

196   replenished with complete medium for 2 days and stained with crystal violet. MOTS-c-treated

197   C2C12 cells showed significantly enhanced proliferative capacity within 2 days (~6-fold) (Fig.

198   5B). Because MOTS-c promotes fat utilization, which may underly its effect on "metabolic

199   flexibility" (Figs. 3F, 4I, J, fig. S5) (*13, 41, 47*), we tested if MOTS-c-treated C2C12 cells could

200   survive on lipids without glucose (0 g/L). As expected, most control cells died without glucose

201   even with lipid supplementation, whereas MOTS-c treatment provided significant protection (~2-

202   fold) (Fig. 5C). Real-time metabolic flux analysis revealed that MOTS-c treatment significantly

203   increased lipid utilization capacity (Fig. 5D) and lipid-dependent glycolysis (fig. S12) in C2C12

204   cells.

205   We previously reported that endogenous MOTS-c translocates to the nucleus to directly regulate

206   adaptive nuclear gene expression in response to cellular stress (*15*). Using fluorescently labeled

207   MOTS-c peptide (MOTS-c-FITC), we confirmed that exogenously treated MOTS-c also

208   dynamically translocated to the nucleus in a time-dependent manner (Fig. 4E) (*15*), indicating a

209   direct nuclear role. We performed RNA-seq on C2C12 cells treated with MOTS-c or vehicle

210    control (10µM) under GR/SD for 48 hours and found (i) clustering by treatment type using a

211    principal component analysis (PCA) (Fig. 5F) and (ii) 69 genes that were differentially regulated

212    at FDR < 5% (Fig. 5G). Further, using the STRING (Search Tool for the Retrieval of Interacting

213    Genes/Proteins) database to assess putative changes in protein-protein interaction networks based

214    on our RNA-seq results, we found that a cluster related to heat-shock responses were prominently

215    regulated by MOTS-c in C2C12 cells under GR/SD; we also identified previously reported MOTS-

216    c targets, including Atf3, Jun, Fosl1, and Mafg (*15*) (Fig. 5H). Consistently, select GO_BP analysis

217    revealed protein regulation as a major target process of MOTS-c in myoblasts (select terms in fig.

218    S13; full results in table S3). To identify common pathways in *in vitro* and *in vivo* models, we

219    overlaid RNA-seq data from MOTS-c-treated (i) old mouse skeletal muscle and (ii) metabolically

220    stressed (GR/SD) C2C12. Select GO_BP analysis revealed several commonly targeted processes,

221    including protein regulation, cellular metabolism, oxidative stress response, and nuclear transport

222    (select terms in Fig. 5I; full results in table S4). Together, these data suggest that MOTS-c

223    improves metabolic homeostasis/flexibility and protein homeostasis in skeletal muscle under

224    exercise-induced stress conditions.

225    Our study shows that exercise induces mtDNA-encoded MOTS-c expression. MOTS-c treatment

226    significantly (i) improved physical performance in young, middle-aged, and old mice, (ii)

227    regulated skeletal muscle metabolism and gene expression, and (iii) enhanced adaptation to

228    metabolic stress in C2C12 cells. Thus, it is plausible that the physiological role of exercise-induced

229    MOTS-c is to promote adaptive responses to exercise-related stress conditions (*e.g.* metabolic

230    imbalance and heat shock) in the skeletal muscle and maintain cellular homeostasis.

231    Mitochondria are strongly implicated in aging at multiple levels (*1, 2, 6-8, 48*). Here, we present

232    evidence that the mitochondrial genome encodes for instructions to maintain physical capacity (*i.e.*

233    performance and metabolism) during aging and thereby increase healthspan. MOTS-c treatment

234    initiated in late-life, proximal to the age at which the lifespan curve rapidly descends for

235    C57BL/6N mice, significantly delayed the onset of age-related physical disabilities, suggesting

236    "compression of morbidity" in later life (*49*). Interestingly, an exceptionally long-lived Japanese

237    population harbors a mitochondrial DNA (mtDNA) SNP (m.1382A>C) that yields a functional

238    variant of MOTS-c (*50, 51*).

239    Our study shows that exogenously treated MOTS-c enters the nucleus and regulates nuclear gene
240    expression, including those involved in heat shock response and metabolism. Thus, age-related
241    gene networks are comprised of integrated factors encoded by both genomes, which entails a bi-
242    genomic basis for the evolution of aging. Although the detailed molecular mechanism(s)
243    underlying the functions of MOTS-c is an active field of research, we provide a "proof-of-
244    principle" study that realizes the mitochondrial genome as a source for instructions that can
245    regulate physical capacity and healthy aging.

246

247

**Materials and Methods**

Mouse Care

All animal work was performed in accordance with the University of Southern California (USC) Institutional Animal Care and Use Committee. MOTS-c (New England Peptide, USA) was administered daily at 5 or 15 mg/kg via intraperitoneal injections. 12-week old male CD-1 (outbred) mice (Charles River, USA), 12-week old male C57BL/6J mice (Jackson Laboratory) and 8- and 18-month old male C57BL/6N mice (National Institute on Aging; NIA) were obtained. All mice were fed either a HFD (60% calories from fat) or matching control diet (Research Diets, USA, #D12492 and D12450J, respectively). NIA mice were sufficiently acclimated for 4 months in our vivarium until they were considered middle-aged (12 mo.) and old (22 mo.) at the start of MOTS-c injections. Body weight and food consumption were recorded daily, while body composition was analyzed twice weekly using an LF90II time-domain NMR minispec (Bruker, USA). After eight weeks of injections (23.5 months of age), mice were transitioned to receive MOTS-c injections three times weekly. No live mouse was censored.


Physical Tests in Mice

*Running Test*: Prior to running training/testing, mice were acclimated to the stationary treadmill apparatus (TSE-Systems, USA) for ten minutes on two consecutive days (Days 1 and 2). Both the high intensity test and training protocols were adapted from previously published protocols (*52*). Running training was given twice on non-consecutive days and consisted of a fixed speed run of 10 m/min for 20 minutes (Days 4 and 6) on a level treadmill. The treadmill test on Day 10 consisted of three stages. Stage one was a five-minute run at 13 m/min. For the next five minutes, the speed was increased by 1 m/min. The mice run at a fixed speed of 18 m/min for the next 30 minutes. Finally, after 40 minutes of total run time, the running speed is increased to 23 m/min until exhaustion is reached. All training and testing were done on a level treadmill. Mice resting on the platform were gently prodded to encourage re-engagement. Any mouse that resisted prodding and remained on the platform for 30 seconds was considered to be exhausted, and time was recorded.

*Walking Test*: When the mice reached 30 months of age, they were no longer capable of performing the same treadmill routine. We developed a measure of mobility in the aged mice consisting of a

277   60 second walking test. The treadmill was set at 13 m/min for 60 seconds. We recorded whether

278   the mouse was able to walk, or not, on the treadmill for 60 seconds, with gentle prodding as needed.

279   Mice remaining on the stationary platform, refusing to engage in the treadmill walking, for more

280   than five seconds were considered to have failed the test.

281   *Rotarod*: The Rotarod test was performed by placing the mice on the apparatus (TSE-Systems),

282   all facing the opposite direction of rotation. The initial speed of rotation was 24 rpm and

283   accelerated at 1 rpm every 10 seconds. Time to fall was recorded for each mouse, and three trials

284   per mouse was run. Mice received no less than five minutes of recovery time between trials.

285   *Grip Strength*: We measured grip strength using a horizontal bar connected to the grip strength

286   meter (TSE-Systems) as a high precision force sensor for the forelimbs. After allowing the mouse

287   to properly grip the bar they were firmly and quickly pulled in the opposite direction. Only trials

288   where the mouse released its paws from the bar simultaneously were counted as successful. Mice

289   underwent three trials, with at least 30 seconds recovery time between trials.

290   *Gait Analysis*: To perform gait analysis, we applied a different color of non-toxic ink (BLICK®,

291   USA) to the front and hind paw of the mice to record footprints. Barriers were constructed to guide

292   the mice to walk straight on the recording paper. The home cage was kept at the end of the

293   recording paper to encourage completion of the test. Only trials in which the mouse made a

294   continuous, direct path to its home cage were counted. Stride length was measured as the average

295   forward movement of three full strides as previously described(*53*).

296   *Cognitive tests*:

297   *Y-maze tests* were performed as previously described (*54*). Briefly, mice were placed in a maze

298   consisting of three arms equally spaced 120° apart. Mice were placed in one arm of the maze and

299   allowed to freely explore the maze for five minutes. Total arm entries and arm choices were

300   recorded for each mouse. An arm entry was defined as a mouse having both front and hind paws

301   entering the arm fully. Percent alternations was defined as an arm choice differing from the

302   previous two compared to the total number of alternation opportunities.

303   *Barnes maze* tests were performed as previously described (*54*). 12-week old male CD-1 mice

304   were tested twice daily for 7 days. Mice were placed in a start chamber in the middle of the maze

305   and allowed to habituate (30 seconds), then the mouse was released to explore the maze and find

306 the escape box (EB). Latency (time to enter the EB) and number of errors (nose pokes and head

307 deflections over false holes) were recorded. A maximum of 2 minutes was allowed for each trial.

308

309 *In Vivo* Metabolism Assessment

310 *Metabolic Cages*: Metabolic activity in mice was measured using the PhenoMaster system (TSE-

311 Systems) equipped to detect indirect calorimetry, measure food and water intake, and monitor

312 activity. Prior to metabolic analysis, mice were housed 3-4 per cage in a facility with a 12:12 hour

313 light- dark cycle (light period 0600-1800) at 24°C. Food and water were available *ad libitum*. For

314 metabolic assessment, nice were moved into individual PhenoMaster cages in an isolated room

315 under the same environmental conditions. Mice were automatedly monitored for 36 hours to record

316 physiological parameters. To measure $O_2$ intake and $CO_2$ production, gas sensors were calibrated

317 prior to the study using primary gas standards of known concentrations of $O_2$, $CO_2$, and $N_2$. Room

318 air was passed through the animal chambers at a rate of 0.5 L/min. Exhaust air from individual

319 cages were sampled at 30-minute intervals for 3 minutes. Sample air was passed through sensors

320 to determine oxygen consumption ($VO_2$) and carbon dioxide production ($VCO_2$). The respiratory

321 exchange ratio (RER) was calculated as the ratio of carbon dioxide produced to oxygen

322 consumption. The PhenoMaster system allows for activity monitoring using a triple beam IR

323 technology system. Breaking the IR beams through movement was considered a "count". The

324 three-beam system allows XYZ monitoring that considers both ambulatory activity around the

325 cage as well as rearing activity. All data are expressed as the mean of three 24-hour acquisition

326 cycles.

327 *Blood glucose*: Blood was collected via a single tail-nick and immediately analyzed using a

328 glucometer (Freestyle, Abbott). Blood collection was performed by trained professionals and in

329 accordance with the University of Southern California Institutional Animal Care and Use

330 Committee.

331

332 Western Blots

333 Protein samples were lysed in 1% Triton X-100 (Thermo Fisher Scientific, USA, #21568-2500)

334 with 1 mM EDTA (Promega Life Sciences, USA, #V4231) and 100 mM Tris-HCl pH 7.5 (Quality

335 Biological, USA, #351-006-101) and protease inhibitors (Roche, Germany, #118636170001) and

336 sonicated using a Sonic Dismembrator (Fisher Scientific, USA). Samples were heated at 95ºC for

337 five minutes. Samples were ran on 4-20% gradient tris-glycine gels (TGX; Bio-Rad, USA, #456-

338 1104) and transferred onto 0.2 µM PVDF membranes (Bio-Rad #162-0184) using a Transblot

339 Turbo semi-dry transfer system (Bio-Rad) at 9 volts for 15 minutes. Membranes were blocked for

340 1 hour using 5% BSA (Akron Biotech, USA, #AK8905-0100) in tris-buffered saline containing

341 0.05% Tween-20 (Bio-Rad #161-0781) and incubated in primary antibodies against MOTS-c

342 (rabbit polyclonal; YenZym, USA) and GAPDH (cat# 5174; Cell Signaling, USA) overnight at

343 4ºC. Secondary HRP-conjugated antibodies (#7074; Cell Signaling, USA) were then added

344 (1:30,000) for one hour at room temperature. Chemiluminescence was detected and imaged using

345 Clarity western ECL substrate (Bio-Rad #1705060) and Chemidoc XRS system (Bio-Rad).

346 Western blots were quantified using ImageJ version 1.52k.

347

348 Cell Studies

349 *Cell culture*: C2C12 cells were cultured in DMEM with 4.5 g/L glucose (Corning, USA #10-017-

350 CV) and 10% FBS (Millipore-Sigma, USA, #F0926-500). All cells were stored at 37°C and 5%

351 $CO_2$. Cells were passaged when they reached 75-80% confluence using TrypLE (Thermo Fisher

352 Scientific #12605-010).

353 *Cell survival assays*: Protection against glucose restriction (GR) and serum deprivation (SD) was

354 tested by culturing cells in DMEM (Thermo Fisher Scientific #11966-025) with 0.5 g/L glucose

355 (Millipore-Sigma #G8769) and 1% FBS. MOTS-c (10µM) or vehicle (PBS). MOTS-c (10µM)

356 was added to the media every 24 hours. After 48 hours of GR/SD, we performed crystal violet

357 (Thermo Fisher Scientific #C581-25) staining as before (*15*) to determine cell survival. We also

358 tested cellular proliferation, following prolonged (7-day) GR/SD (DMEM with 1% FBS and 0.5

359 g/L glucose), as a measure of cellular fitness. In this case, MOTS-c-containing (10µM) media was

360 changed once every two days; no additional MOTS-c supplementation was given between media

361 changes. After 7 days of GR/SD, we returned the cells to full growth media (10% FBS and 4.5 g/L

362 glucose) for 48 hours with MOTS-c (10µM), then stained them with crystal violet. To determine

363 the metabolic flexibility to utilize fatty acids, we cultured cells in DMEM with 1% FBS, 0.5 g/L

364    glucose, and 1% chemically defined lipid mixture (Millipore-Sigma #L0288) for 48 hours, then

365    stained them with crystal violet.

366    *Metabolic flux*: Real-time oxygen consumption and extracellular acidification rates in C2C12

367    myoblasts treated with 16% palmitate-BSA (1mM palmitate conjugated to 0.17mM BSA) or 16%

368    BSA (0.17 mM; Seahorse Bioscience #102720-100) were obtained using the XF96 Bioanalyzer

369    (Seahorse Bioscience) at the USC Leonard Davis School of Gerontology Seahorse Core. All values

370    were normalized to relative protein concentration using a BCA protein assay kit (Thermo Fisher

371    Scientific #23227).

372    *Confocal microscopy*: Confocal images were obtained using a Zeiss Confocal Laser Scanning

373    Microscope 700 (Zeiss, Germany). C2C12 myoblasts were cultured on glass coverslips

374    (Chemglass, USA, #CLS-1760-015). Cells were treated with FITC-MOTS-c (New England

375    Peptide) for either 0 hours (immediate), 30 minutes, 4 hours, or 24 hours. Some cells were left as

376    untreated controls (data not shown). All cells were treated with Hoeschst (Biotium, USA, #40045)

377    for 15 minutes and then washed three times with PBS. Cells were fixed in 10% formalin

378    (Millipore-Sigma #EM-R04586-82) and washed an additional three times in PBS. Coverslips were

379    affixed to glass slides (VWR, USA, #48300-025) using ProLong Gold antifade reagent (Life

380    Technologies Corporation, USA, #P36934).

381

382    <u>Human Studies</u>

383    *Study outline:*

384    Participants gave written consent before the commencement of the study, which was approved by

385    the Northern Health and Disability Ethics Committee (New Zealand) (16/STH/116/AM01). 10

386    sedentary (<4h aerobic exercise/week) healthy young males (24.5 ± 3.7 years old and BMI 24.1 ±

387    2.1) were recruited to take part in a two-visit exercise trial. Recruited participants were free of

388    cardiovascular, metabolic and blood diseases and were not taking any medication or supplements.

389    The trial was separated into two visits, each involving exercise bouts that were carried out on an

390    electromagnetically braked cycle ergometer (Velotron, RacerMate, USA).

391  *Determination of peak oxygen uptake (VO₂peak) and maximal power output (visit 1)*: Peak oxygen
392  uptake was determined using a ramped cycling exercise protocol. Prior to testing, participants
393  warmed up for five minutes at a self-selected workload between 60 and 80W. The ramp protocol
394  began at 60W, with the cycling power output set to increase by 1W every 4 seconds (15W/min)
395  continuously until the participant was unable to maintain cycling workload (cycling
396  cadence<minimum 60 revolutions per minute) or maximal volitional fatigue was reached. Mean
397  Peak oxygen uptake of participants was reported as $38.4 \pm 7.3$ ml.kg.min.

398  *Acute high intensity cycling exercise session (visit 2)*: Prior to visit 2, participants were asked to
399  fast overnight (from 10PM) and were instructed to abstain from physical activity for at least 48h
400  prior. Upon arrival to the laboratory, participants lay supine for 15-minutes and then had an
401  intravenous cannula inserted into a forearm vein. A resting plasma sample was collected followed
402  by a pre-exercise muscle biopsy taken from the vastus lateralis muscle (quadriceps muscle).
403  Approximately 10-minutes later, participants completed ten, 60-second cycling intervals at
404  individually-specified peak power workloads (determined from peak oxygen uptake test) followed
405  by 75-seconds of rest/low intensity cycling (<30W) per interval as previously described (*55*). A
406  mid-exercise blood sample was taken following the completion of the 5th exercise interval as well
407  as immediately following the completion of the exercise bout. In addition, an immediately-post
408  exercise muscle biopsy was taken (within ~5-minutes of completion of the exercise bout).
409  Participants remained supine and resting in the procedure bed for a 4-hour recovery period.
410  Following four-hours of recovery, a final blood and muscle biopsy sample was collected.

411  *Muscle biopsy and blood sampling*: Muscle biopsies were extracted under local anesthesia (1%
412  xylocaine) using the Bergstrom needle with manual suction technique(*56*). Biopsies were snap-
413  frozen in liquid nitrogen and stored at −80°C until analyzed. Blood was drawn through a 20-gauge
414  cannula, collected in 10-mL EDTA vacutainers and then centrifuged immediately upon collection
415  at 4°C at 2,000 g for 10 minutes. Plasma was extracted and then stored at −80°C until further
416  analysis using an in-house ELISA as described before (*13*). Human skeletal muscle was processed
417  for western blotting by soaking the samples in lysis buffer (above) and minced using a razor blade.
418  Once the sample was evenly minced, we proceeded with the Sonic Dismembrator step as described
419  above.

420

Liquid Chromatography-Mass Spectrometry Metabolomics

Metabolites were extracted from randomly selected tissue samples by adding 1 mL of 80:20 methanol:water solution on dry ice. Samples were incubated at -80C for 4 hours and centrifuged at 4C for 5 minutes at 15k rpm. Supernatants were transferred into LoBind Eppendorf microcentrifuge tubes and the cell pellets were re-extracted with 200 μL ice-cold 80% MeOH, spun down and the supernatants were combined. Metabolites were dried at room temperature under vacuum and re-suspended in water for injection.

Samples were randomized and analyzed on a Q-Exactive Plus hybrid quadrupole-Orbitrap mass spectrometer coupled to an UltiMate 3000 UHPLC system (Thermo Scientific). The mass spectrometer was run in polarity switching mode (+3.00 kV/-2.25 kV) with an m/z window ranging from 65 to 975. Mobile phase A was 5 mM NH4AcO, pH 9.9, and mobile phase B was acetonitrile. Metabolites were separated on a Luna 3 μm NH2 100 Å (150 × 2.0 mm) column (Phenomenex). The flowrate was 300 μl/min, and the gradient was from 15% A to 95% A in 18 min, followed by an isocratic step for 9 min and re-equilibration for 7 min. All samples were injected twice for technical duplicates. Metabolites were detected and quantified as area under the curve based on retention time and accurate mass ($\leq$ 5 ppm) using the TraceFinder 3.3 (Thermo Scientific) software.

RNA-seq

*RNA purification from tissue and cells*: Total RNA extraction from skelatal muscle tissue or C2C12 mouse myoblasts was done using TRI Reagent (Millipore-Sigma #T9424). Muscle tissue samples were flash-frozen in liquid nitrogen until further processing. Tissues were resuspended in 600μL of TRI Reagent, then homogenized on Lysing Matrix D 2mL tubes (MP Biomedicals) on a BeadBug homogenizer (Benchmark Scientific). For both skeletal muscle and C2C12 cells, total RNA was purified using the Direct-zol RNA MiniPrep (Zymo Research #R2052).

*RNA-seq library preparation*: Total RNA was subjected to rRNA depletion using the NEBNext rRNA Depletion Kit (New England Biolabs), according to the manufacturer's protocol. Strand specific RNA-seq libraries were then constructed using the SMARTer Stranded RNA-Seq Kit (Clontech # 634839), according to the manufacturer's protocol. Based on rRNA-depleted input

450    amount, 13-15 cycles of amplification were performed to generate RNA-seq libraries. Paired-end

451    150bp reads were sent for sequencing on the Illumina HiSeq-Xten platform at the Novogene

452    Corporation (USA). The raw sequencing data was deposited to the NCBI Sequence Read Archive

453    (accession: PRJNA556045). The resulting data was then analyzed with a standardized RNA-seq

454    data analysis pipeline (described below).

455    *RNA-seq analysis pipeline*: To avoid the mapping issues due to overlapping sequence segments in

456    paired end reads, reads were hard trimmed to 75bp using the Fastx toolkit v0.0.13.  Reads were

457    then further quality-trimmed using Trimgalore 0.4.4 (github.com/FelixKrueger/TrimGalore) to

458    retain high-quality bases with Phred score > 20. All reads were also trimmed by 6 bp from their 5'

459    end to avoid poor qualities or biases. cDNA sequences of protein coding and lincRNA genes were

460    obtained through ENSEMBL Biomart for the GRCm38 build of the mouse genome (Ensemble

461    release v94). Trimmed reads were mapped to this reference using kallisto 0.43.0-1 and the –fr-

462    stranded option (*57*). All subsequent analyses were performed in the R statistical software

463    (https://cran.r-project.org/).

464    Read counts were imported into R, and summarized at the gene level, to estimate differential gene

465    expression as a function of age.

466    Because of high sample variability, we used surrogate variable analysis to remove experimental

467    noise from the muscle RNA-seq dataset (*58*). R package 'sva' v3.24.4 (*59*) was used to estimate

468    surrogate variable, and the effects of surrogate variables were regressed out using 'limma'.

469    Corrected read counts were then used for downstream analyses.

470    DEseq2 normalized fold-changes were then used to estimate differential gene expression between

471    control and MOTS-c treated muscle or cell samples using the 'DESeq2' R package (DESeq2

472    1.16.1)(*60*). The heatmap of expression across samples for significant genes (Fig. 4G) was plotted

473    using the R package 'pheatmap' 1.0.10 (Raivo Kolde, 2015-12-11; https://CRAN.R-

474    project.org/package=pheatmap). Putative protein-protein interaction was derived using the

475    STRING (Search Tool for the Retrieval of Interacting Genes/Proteins) database version 11.0 (*61*)

476    (https://string-db.org/).

477

478

479    Functional enrichment analysis

480    To perform functional enrichment analysis, we used the Gene Set Enrichment Analysis paradigm

481    through its implementation in the R package 'ClusterProfiler' v3.10.1 (*62*), and Bioconductor

482    annotation package 'org.Mm.eg.db' v3.7.0. Balloon plots representing the output were generated

483    using R packages 'ggplot2' v3.1.0 and 'scales' 1.0.0.

484

485    Principal Component Analysis

486    *Metabolites*: Principal component analysis (PCA) was performed using the mean-centered matrix

487    of metabolite values per each mouse. Principal components that separated sample groups were

488    identified with visual inspection.  Loadings from principal components that stratify experimental

489    samples versus controls were then queried against metabolic pathways using a Kolmogorov-

490    Smirnov statistic against the expected distribution of metabolites. Metabolic pathway enrichment

491    analysis (gene set enrichment analysis, GSEA) (*63*) were performed using 28 metabolic pathways

492    defined by the Kyoto Encyclopedia of Genes and Genomes (KEGG) database using pathways with

493    four or more measured metabolites.

494    *RNA-seq*: PCA was performed using the R base package function 'prcomp'. The first 2 principal

495    components were used.

496

497    Quantification and Statistical Analysis

498    Unless otherwise noted, statistical significance was determined using the Student $t$-test. Statistical

499    tests were performed using GraphPad Prism version 8.1.2. Results of $t$-tests are indicated in all

500    figures as $*p<0.05$, $** p<0.01$, $***p <0.001$ and $ns$ for not significant ($p>0.05$).

501    The RNA-seq analytical code will be made available on the Benayoun lab github

502    (https://github.com/BenayounLaboratory/MOTSc_Exercise).

503

504

505

**Figure Legends:**

**Fig. 1. MOTS-c responds to and regulates exercise in young subjects.** (**A**) Schedule of exercise on a stationary bicycle and blood and skeletal muscle collection in young male subjects (n=10). (**B, C**) Representative western blot of MOTS-c from skeletal muscle and quantification (**D**) Quantification of serum MOTS-c levels by ELISA. Data expressed as mean +/- SEM. Wilcoxon matched-pairs signed rank test was used for (**C, D**).

**Fig. 2. MOTS-c treatment increases physical capacity in young mice regardless of diet.** (**A-C**) Treadmill performance of 12-week old male CD-1 (outbred) mice fed a normal diet (n=5-6); (**A**) running curves, (**B**) total time on treadmill, (**C**) total distance ran, and (**D**) percent capable of reaching the highest speed (sprint). (**E-H**) Treadmill performance of 12-week old male C57BL/6J (inbred) mice fed a HFD (n=8); (**E**) running curves, (**F**) total time on treadmill (**G**) total distance ran (**H**) percent capable of reaching the highest speed (final stage). (**I**) PCA and MSEA on metabolomic data from skeletal muscle and liver of C57BL/6J mice that were fed a HFD, treated with MOTS-c, and exercised. Data expressed as mean +/- SEM. Log-rank (Mantel-Cox) test was used for (**A, E**). Otherwise, all statistics were performed using the Student's *t*-test. *$P<0.05$, ** $P<0.01$, *** $P<0.001$.

**Fig. 3. Acute MOTS-c treatment enhances physical capacity in old mice.** (**A**) Schedule of MOTS-c treatment and assays in middle-aged and old C57BL/6N mice (n=10 and 16-19, respectively), including (**B**) treadmill running curves, (**C**) total time on treadmill, (**D**) total distance ran on treadmill, and (**E**) percent capable of reaching the highest speed on a treadmill (final stage). (**F**) Respiratory exchange ratio (RER) following 2 weeks of daily MOTS-c injection (n=4). (**G, H**) Skeletal muscle from treadmill-exercised old mice (22.5 months) treated daily with MOTS-c (15 mg/kg/day) for 2 weeks (n=10) were subject to (**G**) metabolomics and analyzed using PCA and MSEA and (**H**) GSEA analysis of muscle RNA-seq analysis. Balloon plots of select enriched terms using Gene Ontology Biological Process (GO_BP) database at false discovery rate (FDR) < 15%. Full GSEA results are available in table S1. Data expressed as mean +/- SEM. Log-rank (Mantel-Cox) test was used for (**B**) and two-way ANOVA (repeated measures) was used for (**F**). GSEA

535    statistics from R package 'clusterProfiler' were used for (**H**). Otherwise, all statistics were

536    performed using the Student's *t*-test. *$P<0.05$, ** $P<0.01$, *** $P<0.001$.

537

538    **Fig. 4. MOTS-c regulates aging metabolism and healthspan.** Life-long measurements on male

539    C57BL6/N mice treated intermittently (3x/week) with MOTS-c (15 mg/kg/day) starting at middle

540    and old age (13.5 and 23.5 mo.) as described in Fig. 2a (n=16-19). (**A**) grip strength test (n=11),

541    (**B**) gait analysis (stride length) (n=5), (**C**) 60-second walking test (n=11-12), and (**D**) blood

542    glucose levels (n=11). (**E, F**) Body weight (**E**) as a function of time and (**F**) the total sum ($\sum$); (**G,**

543    **H**) Food intake (**G**) as a function of time and (**H**) the total sum ($\sum$); (**I, J**) Percent fat mass (**I**) as a

544    function of time and (**J**) the total sum ($\sum$); (**K, L**) Percent lean mass (**K**) as a function of time and

545    (**L**) the total sum ($\sum$). (**M**) Lifespan curve; $P=0.05$ until 31.8 months of age. Overall curve trended

546    towards increased median and maximum lifespan ($P=0.23$). Data expressed as mean +/- SEM.

547    Log-rank (Mantel-Cox) test was used for (**M**). Otherwise, all statistics were performed using the

548    Student's *t*-test. *$P<0.05$, ** $P<0.01$, *** $P<0.001$.

549

550    **Fig. 5. MOTS-c regulates myoblast gene expression and enhances adaptation to metabolic**

551    **stress.** (**A-C**) Survival of MOTS-c-treated (10µM; equal-volume vehicle control) C2C12

552    myoblasts assessed by crystal violet staining following (**A**) 48 hours of glucose restriction (GR;

553    0.5 g/L) and serum deprivation (SD; 1% FBS) with MOTS-c treated only once initially (n=12),

554    (**B**) 7 days of GR/SD with daily MOTS-c treatment, followed by a 2-day recovery in full media

555    with MOTS-c (n=10), and (**C**) 48 hours of complete GR (0 g/L) with chemically-defined lipid

556    supplementation and daily MOTS-c treatment (n=6). (**D**) Real-time oxygen consumption rate

557    (OCR) in response to fatty acid (palmitate-BSA) in C2C12 myoblasts treated with MOTS-c

558    (10µM) for 48 hours (n=11-12). (**E**) Time-dependent subcellular localization pattern of

559    exogenously treated MOTS-c-FITC (10µM) in C2C12 myoblasts. Scale bar: 10µm. (**F-I**) RNA-

560    seq was performed on C2C12 myoblasts following 48 hours of GR/SD with/without a unique

561    initial MOTS-c (10µM) treatment (n=6). (**F**) Principle Component Analysis (PCA) and (**G**)

562    heatmap of significantly differentially regulated genes by MOTS-c at false discovery rate (FDR)

563    < 5% by DESeq2 analysis. (**H**) Protein-protein interaction network analysis based on genes that

564    were significantly differentially regulated by MOTS-c (FDR < 5%) using the STRING (Search

565     Tool for the Retrieval of Interacting Genes/Proteins) database version 11.0 (*61*). (**I**) Balloon plots

566     of common biological processes derived from RNA-seq data between MOTS-c-treated (i) skeletal

567     muscle from old mice (see Fig. 2) and (ii) C2C12 myoblasts, based on gene set enrichment analysis

568     (GSEA) using gene ontology biological process (GO_BP) (select gene sets; FDR < 15%). Data

569     expressed as mean +/- SEM. Student's *t*-test. *$P<0.05$, ** $P<0.01$, *** $P<0.001$

570

581

582     **Author contributions:** J.C.R., T.L.M., B.A.B., P.C., N.A.G., D.C-S., and C.L. conceived the

583     experiments. J.C.R., J.S.T.W., B.A.B., R.L., R.W.L., J.H.J., C.J.M., and D.C-S. performed

584     experiments. J.C.R., T.L.M., J.S.T.W., B.A.B., R.L., R.W.L., P.C., N.A.G., J.H.J., and C.L.

585     analyzed the data. J.C.R. and C.L. wrote the manuscript.

586

587     **Competing interests:** P.C. and C.L. are consultants and shareholders of CohBar, Inc. All other

588     authors declare no competing interests.

589

590     **Data and materials availability:** All data are available in the main manuscript and Extended Data

591     material. RNA-seq data have been uploaded to the NCBI SRA database (accession:

592     PRJNA556045).

593

## References:
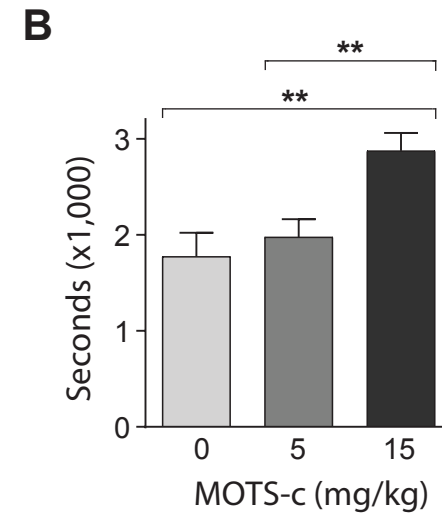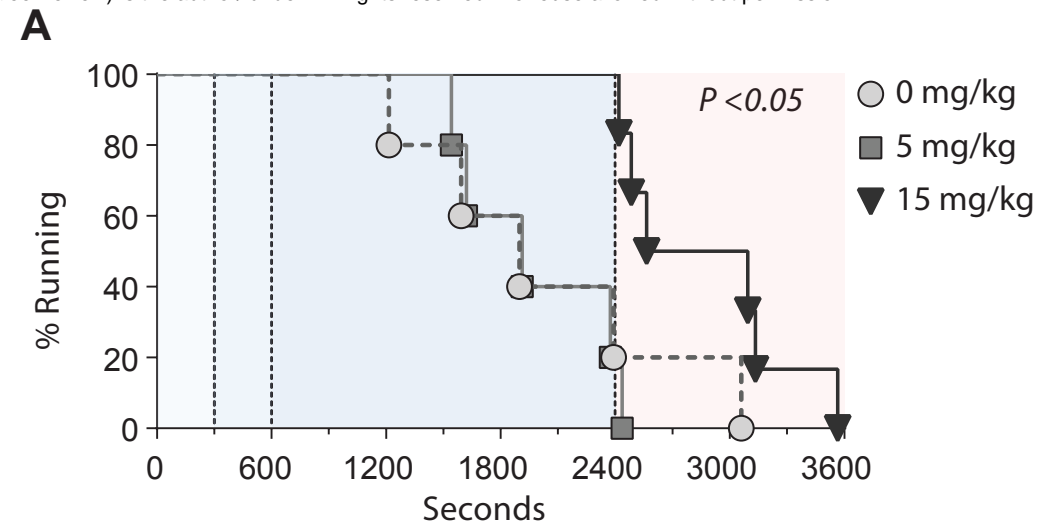
1. C. Lopez-Otin, M. A. Blasco, L. Partridge, M. Serrano, G. Kroemer, The hallmarks of aging. *Cell* **153**, 1194-1217 (2013).
2. C. Lopez-Otin, L. Galluzzi, J. M. Freije, F. Madeo, G. Kroemer, Metabolic Control of Longevity. *Cell* **166**, 802-821 (2016).
3. A. Bratic, N. G. Larsson, The role of mitochondria in aging. *J Clin Invest* **123**, 951-957 (2013).
4. S. Hill, H. Van Remmen, Mitochondrial stress signaling in longevity: A new role for mitochondrial function in aging. *Redox biology* **2**, 936-944 (2014).
5. Martin B. Jensen, H. Jasper, Mitochondrial Proteostasis in the Control of Aging and Longevity. *Cell metabolism* **20**, 214-225 (2014).
6. Y. Wang, S. Hekimi, Mitochondrial dysfunction and longevity in animals: Untangling the knot. *Science* **350**, 1204-1207 (2015).
7. T. E. S. Kauppila, J. H. K. Kauppila, N.-G. Larsson, Mammalian Mitochondria and Aging: An Update. *Cell metabolism* **25**, 57-71 (2017).
8. J. Y. Jang, A. Blum, J. Liu, T. Finkel, The role of mitochondria in aging. *J Clin Invest* **128**, 3662-3670 (2018).
9. P. M. Quirós, A. Mottis, J. Auwerx, Mitonuclear communication in homeostasis and stress. *Nature Reviews Molecular Cell Biology* **17**, 213-226 (2016).
10. J. Durieux, S. Wolff, A. Dillin, The cell-non-autonomous nature of electron transport chain-mediated longevity. *Cell* **144**, 79-91 (2011).
11. C. Lee, K. Yen, P. Cohen, Humanin: a harbinger of mitochondrial-derived peptides? *Trends in endocrinology and metabolism: TEM*,  (2013).
12. S.-J. Kim, J. Xiao, J. Wan, P. Cohen, K. Yen, Mitochondrially derived peptides as novel regulators of metabolism. *The Journal of Physiology* **595**, 6613-6621 (2017).
13. C. Lee *et al.*, The mitochondrial-derived peptide MOTS-c promotes metabolic homeostasis and reduces obesity and insulin resistance. *Cell Metab* **21**, 443-454 (2015).
14. K. Zarse, M. Ristow, A mitochondrially encoded hormone ameliorates obesity and insulin resistance. *Cell Metab* **21**, 355-356 (2015).
15. K. H. Kim, J. M. Son, B. A. Benayoun, C. Lee, The Mitochondrial-Encoded Peptide MOTS-c Translocates to the Nucleus to Regulate Nuclear Gene Expression in Response to Metabolic Stress. *Cell metabolism* **28**, 516-524 e517 (2018).
16. K. C. Mangalhara, G. S. Shadel, A Mitochondrial-Derived Peptide Exercises the Nuclear Option. *Cell Metab* **28**, 330-331 (2018).
17. W. Wong, Going nuclear with stress. *Science Signaling* **11**,  (2018).
18. P. P. Singh, B. A. Demmitt, R. D. Nath, A. Brunet, The Genetics of Aging: A Vertebrate Perspective. *Cell* **177**, 200-220 (2019).
19. L. Fontana, L. Partridge, V. D. Longo, Extending healthy life span--from yeast to humans. *Science* **328**, 321-326 (2010).
20. B. K. Kennedy *et al.*, Geroscience: Linking Aging to Chronic Disease. *Cell* **159**, 709-713 (2014).
21. J. Campisi *et al.*, From discoveries in ageing research to therapeutics for healthy ageing. *Nature* **571**, 183-192 (2019).
22. D. E. Gottschling, T. Nyström, The Upsides and Downsides of Organelle Interconnectivity. *Cell* **169**, 24-34 (2017).
23. O. Matilainen, P. M. Quirós, J. Auwerx, Mitochondria and Epigenetics – Crosstalk in Homeostasis and Stress. *Trends in Cell Biology* **27**, 453-463 (2017).
24. M. Ramanjaneya *et al.*, Mitochondrial-Derived Peptides Are Down Regulated in Diabetes Subjects. *Frontiers in Endocrinology* **10**,  (2019).
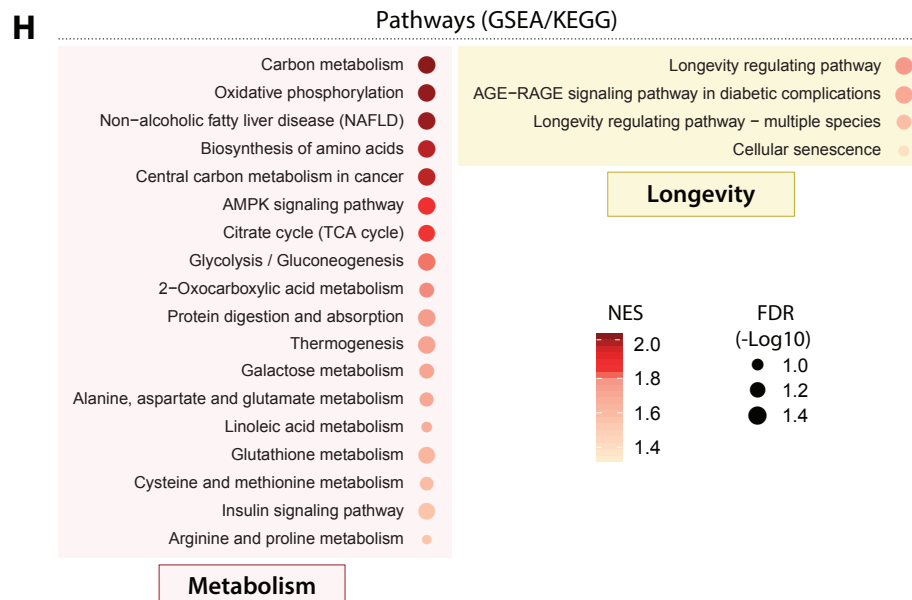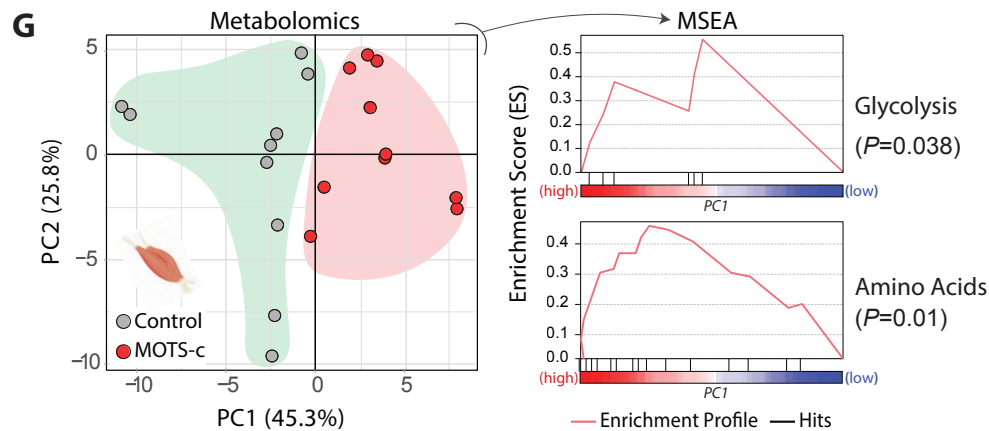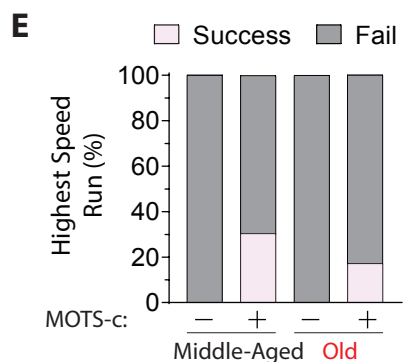
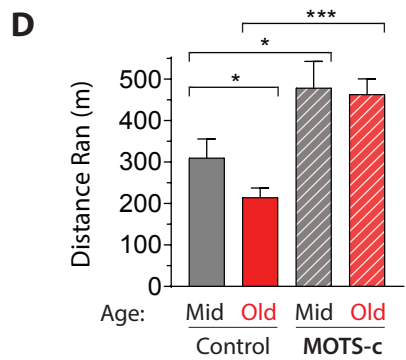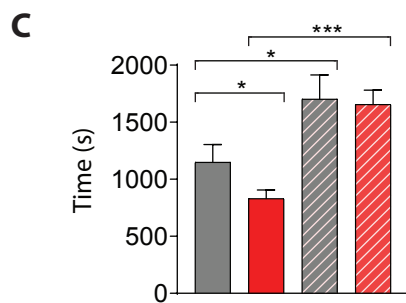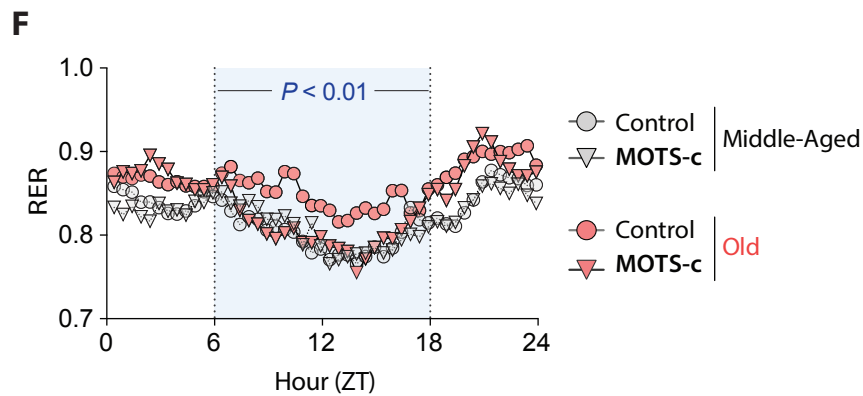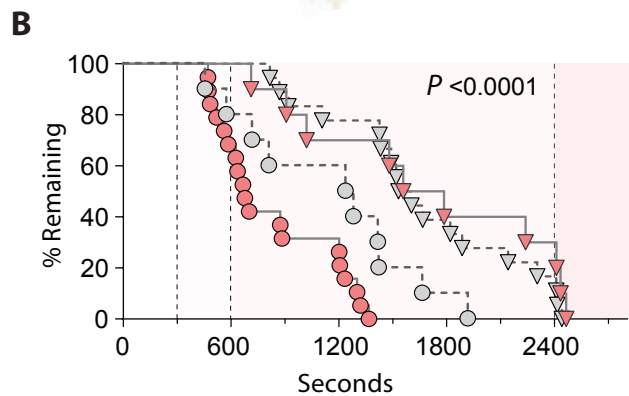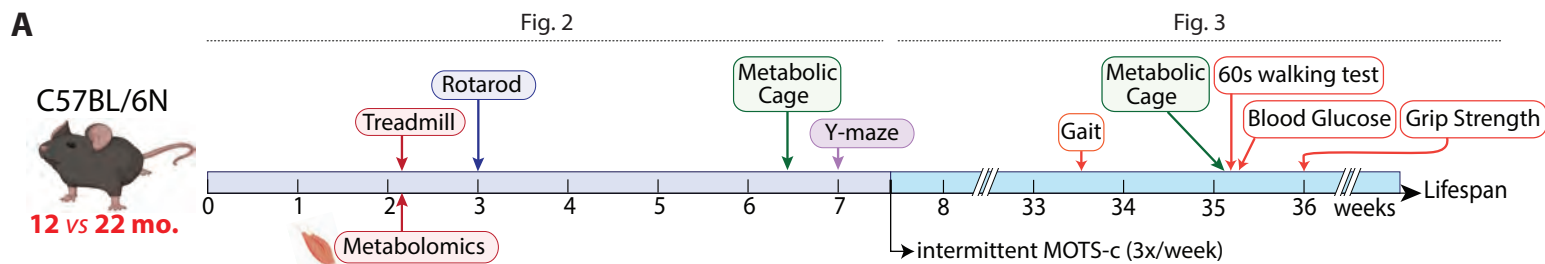641 25. C. Q. Y. Yong, B. L. Tang, A Mitochondrial Encoded Messenger at the Nucleus. *Cells* **7**, (2018).

642 26. R. Alis, A. Lucia, J. R. Blesa, F. Sanchis-Gomar, The role of mitochondrial derived peptides (MDPs)
643 in metabolism. *Journal of cellular physiology* **230**, 2903-2904 (2015).

644 27. S. Li, I. Laher, Exercise Pills: At the Starting Line. *Trends in pharmacological sciences*, (2015).

645 28. A. Knoop, A. Thomas, M. Thevis, Development of a mass spectrometry based detection method
646 for the mitochondrion-derived peptide MOTS-c in plasma samples for doping control purposes.
647 *Rapid Commun Mass Spectrom* **33**, 371-380 (2019).

648 29. B. H. Goodpaster, L. M. Sparks, Metabolic Flexibility in Health and Disease. *Cell Metabolism* **25**,
649 1027-1036 (2017).

650 30. R. L. Smith, M. R. Soeters, R. C. I. Wüst, R. H. Houtkooper, Metabolic Flexibility as an Adaptation
651 to Energy Resources and Requirements in Health and Disease. *Endocrine Reviews* **39**, 489-517
652 (2018).

653 31. N. Barzilai, J. P. Crandall, S. B. Kritchevsky, M. A. Espeland, Metformin as a Tool to Target Aging.
654 *Cell Metabolism* **23**, 1060-1065 (2016).

655 32. M. Kaeberlein, P. S. Rabinovitch, G. M. Martin, Healthy aging: The ultimate preventative
656 medicine. *Science* **350**, 1191-1193 (2015).

657 33. N. L. Nadon, R. Strong, R. A. Miller, D. E. Harrison, NIA Interventions Testing Program:
658 Investigating Putative Aging Intervention Agents in a Genetically Heterogeneous Mouse Model.
659 *EBioMedicine* **21**, 3-4 (2017).

660 34. D. E. Harrison *et al.*, Rapamycin fed late in life extends lifespan in genetically heterogeneous
661 mice. *Nature* **460**, 392-395 (2009).

662 35. K. Mao *et al.*, Late-life targeting of the IGF-1 receptor improves healthspan and lifespan in
663 female mice. *Nature Communications* **9**, (2018).

664 36. P. D. Neufer *et al.*, Understanding the Cellular and Molecular Mechanisms of Physical Activity-
665 Induced Health Benefits. *Cell Metab* **22**, 4-11 (2015).

666 37. L. R. Cataldo, R. Fernandez-Verdejo, J. L. Santos, J. E. Galgani, Plasma MOTS-c levels are
667 associated with insulin sensitivity in lean but not in obese individuals. *J Investig Med* **66**, 1019-
668 1022 (2018).

669 38. C. Du *et al.*, Circulating MOTS-c levels are decreased in obese male children and adolescents and
670 associated with insulin resistance. *Pediatr Diabetes*, (2018).

671 39. Q. Li *et al.*, Earlier changes in mice after D-galactose treatment were improved by mitochondria
672 derived small peptide MOTS-c. *Biochemical and biophysical research communications*, (2019).

673 40. H. Lu *et al.*, MOTS-c peptide regulates adipose homeostasis to prevent ovariectomy-induced
674 metabolic dysfunction. *J Mol Med (Berl)*, (2019).

675 41. M. Ramanjaneya *et al.*, Lipids and insulin regulate mitochondrial-derived peptide (MOTS-c) in
676 PCOS and healthy subjects. *Clinical Endocrinology*, (2019).

677 42. John, M. Hargreaves, Michael, Juleen, Integrative Biology of Exercise. *Cell* **159**, 738-749 (2014).

678 43. B. Egan, Juleen, Exercise Metabolism and the Molecular Regulation of Skeletal Muscle
679 Adaptation. *Cell metabolism* **17**, 162-184 (2013).

680 44. L. Packer, E. Cadenas, K. J. A. Davies, Free radicals and exercise: An introduction. *Free Radical
681 Biology and Medicine* **44**, 123-125 (2008).

682 45. T. L. Merry, M. Ristow, Do antioxidant supplements interfere with skeletal muscle adaptation to
683 exercise training? , n/a-n/a (2015).

684 46. D. Chrétien *et al.*, Mitochondria are physiologically maintained at close to 50 °C. *PLOS Biology*
685 **16**, e2003992 (2018).

686 47. S. J. Kim *et al.*, The mitochondrial-derived peptide MOTS-c is a regulator of plasma metabolites
687 and enhances insulin sensitivity. *Physiological Reports* **7**, (2019).

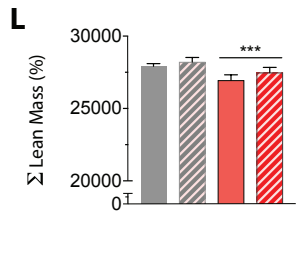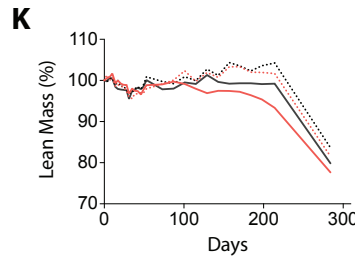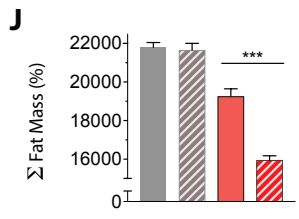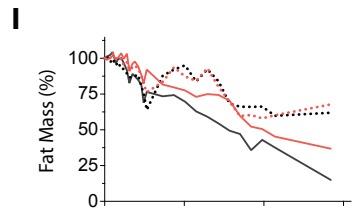688 48. J. M. Son, C. Lee, Mitochondria: multifaceted regulators of aging. *BMB Reports* **52**, 13-23 (2019).

689  49.  E. M. Crimmins, Lifespan and Healthspan: Past, Present, and Promise. *The Gerontologist* **55**, 901-
690        911 (2015).
691  50.  H. Zempo *et al.*, Relation between type 2 diabetes and m. 1382 A> C polymorphism which
692        occurs amino acid replacement (K14Q) of mitochondria-derived MOTS-c. *The FASEB Journal* **30**,
693        956.951-956.951 (2016).
694  51.  N. Fuku *et al.*, The mitochondrial-derived peptide MOTS-c: a player in exceptional longevity?
695        *Aging Cell* **14**, 921-923 (2015).
696  52.  A. Das *et al.*, Impairment of an Endothelial NAD(+)-H2S Signaling Network Is a Reversible Cause
697        of Vascular Aging. *Cell* **173**, 74-89 e20 (2018).
698  53.  R. J. Carter, J. Morton, S. B. Dunnett, Motor coordination and balance in rodents. *Curr Protoc*
699        *Neurosci* **Chapter 8**, Unit 8 12 (2001).
700  54.  S. Brandhorst *et al.*, A Periodic Diet that Mimics Fasting Promotes Multi-System Regeneration,
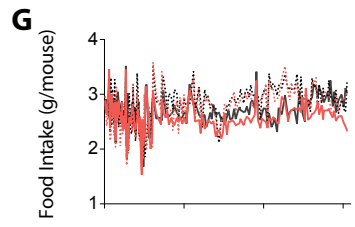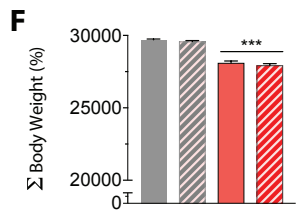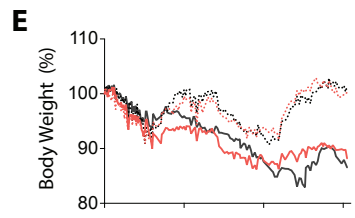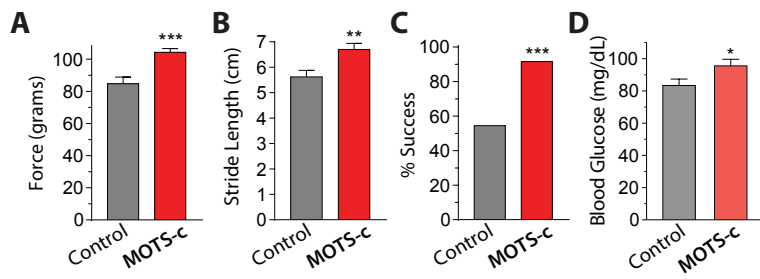701        Enhanced Cognitive Performance, and Healthspan. *Cell Metabolism* **22**, 86-99 (2015).
702  55.  C. P. Hedges *et al.*, Peripheral blood mononuclear cells do not reflect skeletal muscle
703        mitochondrial function or adaptation to high-intensity interval training in healthy young men. *J*
704        *Appl Physiol (1985)* **126**, 454-461 (2019).
705  56.  J. Bergstrom, Percutaneous needle biopsy of skeletal muscle in physiological and clinical
706        research. *Scand J Clin Lab Invest* **35**, 609-616 (1975).
707  57.  N. L. Bray, H. Pimentel, P. Melsted, L. Pachter, Near-optimal probabilistic RNA-seq
708        quantification. *Nature Biotechnology* **34**, 525-527 (2016).
709  58.  J. T. Leek, J. D. Storey, Capturing Heterogeneity in Gene Expression Studies by Surrogate Variable
710        Analysis. *PLoS Genetics* **3**, e161 (2007).
711  59.  J. T. Leek *et al.*, sva: Surrogate Variable Analysis. R package version 3.32.1., (2019).
712  60.  M. I. Love, W. Huber, S. Anders, Moderated estimation of fold change and dispersion for RNA-
713        seq data with DESeq2. *Genome Biology* **15**, (2014).
714  61.  D. Szklarczyk *et al.*, STRING v11: protein–protein association networks with increased coverage,
715        supporting functional discovery in genome-wide experimental datasets. *Nucleic Acids Research*
716        **47**, D607-D613 (2019).
717  62.  G. Yu, L.-G. Wang, Y. Han, Q.-Y. He, clusterProfiler: an R Package for Comparing Biological
718        Themes Among Gene Clusters. *OMICS: A Journal of Integrative Biology* **16**, 284-287 (2012).
719  63.  A. Subramanian *et al.*, Gene set enrichment analysis: A knowledge-based approach for
720        interpreting genome-wide expression profiles. *Proceedings of the National Academy of Sciences*
721        **102**, 15545-15550 (2005).

722

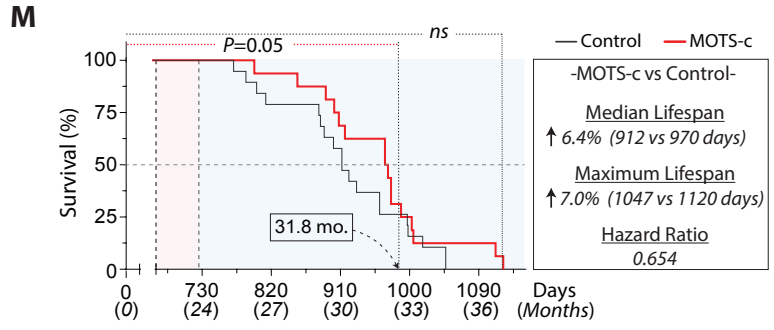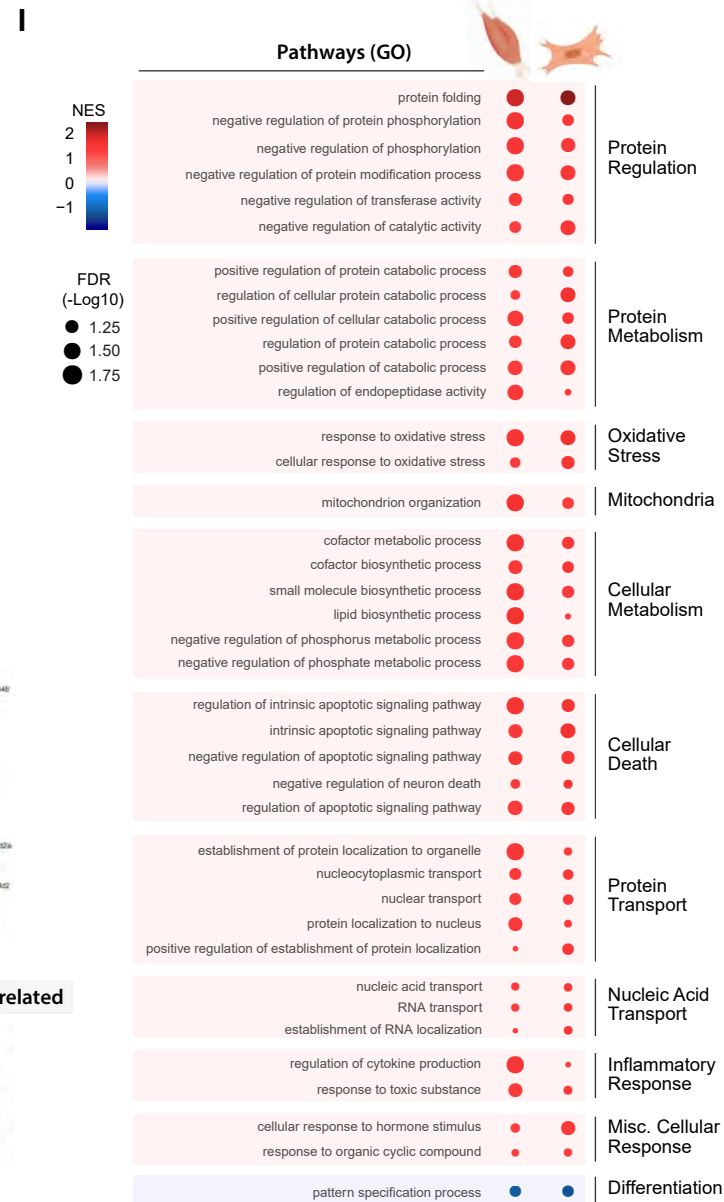**A**

VO₂ Peak

10 x 60s (@ VO₂ Peak)
75s rest

0  48 hrs

4 hrs

Pre    Mid    Post    4-hr

**B**

IB: **MOTS-c**    Pre  Post  4-hr
IB: GAPDH

**C**

Relative MOTS-c

sk. muscle

Pre    Post    4 Hour

**D**

plasma

Pre    Mid    Post    4 Hour

**A**

Fig. 2 | Fig. 3

C57BL/6N

12 vs 22 mo.

Treadmill  Rotarod  Metabolic Cage  Y-maze  Gait  Metabolic Cage  60s walking test  Blood Glucose  Grip Strength

Metabolomics

0 1 2 3 4 5 6 7 8 33 34 35 36 weeks → Lifespan

→ intermittent MOTS-c (3x/week)

**B**

P <0.0001

% Remaining

0 600 1200 1800 2400
Seconds

**C**

Time (s)

*** * *

**D**

Distance Ran (m)

* * ***

Age: Mid Old Mid Old
Control  MOTS-c

**E**

Success  Fail

Highest Speed Run (%)

MOTS-c:  −  +  −  +
Middle-Aged  Old

**F**

P < 0.01

RER

0 6 12 18 24
Hour (ZT)

Control | Middle-Aged
MOTS-c
Control | Old
MOTS-c

**G**

Metabolomics

MSEA

PC2 (25.8%)

PC1 (45.3%)

Control  MOTS-c

Enrichment Score (ES)

Glycolysis (P=0.038)

(high)  PC1  (low)

Amino Acids (P=0.01)

(high)  PC1  (low)

Enrichment Profile  Hits

**H**

Pathways (GSEA/KEGG)

Carbon metabolism
Oxidative phosphorylation
Non−alcoholic fatty liver disease (NAFLD)
Biosynthesis of amino acids
Central carbon metabolism in cancer
AMPK signaling pathway
Citrate cycle (TCA cycle)
Glycolysis / Gluconeogenesis
2−Oxocarboxylic acid metabolism
Protein digestion and absorption
Thermogenesis
Galactose metabolism
Alanine, aspartate and glutamate metabolism
Linoleic acid metabolism
Glutathione metabolism
Cysteine and methionine metabolism
Insulin signaling pathway
Arginine and proline metabolism

**Metabolism**

Longevity regulating pathway
AGE−RAGE signaling pathway in diabetic complications
Longevity regulating pathway − multiple species
Cellular senescence

**Longevity**

NES
2.0
1.8
1.6
1.4

FDR (-Log10)
1.0
1.2
1.4

**A** Force (grams) — Control, MOTS-c ***

**B** Stride Length (cm) — Control, MOTS-c **

**C** % Success — Control, MOTS-c ***

**D** Blood Glucose (mg/dL) — Control, MOTS-c *

**E** Body Weight (%) vs Days

**F** Σ Body Weight (%) ***

**G** Food Intake (g/mouse) vs Days

**H** Σ Food Intake * ***

**I** Fat Mass (%) vs Days

**J** Σ Fat Mass (%) ***

**K** Lean Mass (%) vs Days

**L** Σ Lean Mass (%) ***

······· Middle-Aged Control          ▓ Middle-Aged Control
······· Middle-Aged **MOTS-c**       ▒ Middle-Aged **MOTS-c**
——— Old Control                      ▓ Old Control
——— Old **MOTS-c**                   ▒ Old **MOTS-c**

**M** Survival (%) vs Days (Months)

Control — MOTS-c

P=0.05     ns

31.8 mo.

-MOTS-c vs Control-

Median Lifespan
↑ 6.4% (912 vs 970 days)

Maximum Lifespan
↑ 7.0% (1047 vs 1120 days)

Hazard Ratio
0.654

Days: 0 (0), 730 (24), 820 (27), 910 (30), 1000 (33), 1090 (36)

**A** C2C12
Energy Deficit Stress (Glc/Serum Restrict)
⊖ MOTS-c    ⊕ MOTS-c
48 hrs

Rel. Crystal Violet (OD570)
***
Control    MOTS-c

**B** Energy Deficit Stress (Glc/Serum Restrict)
⊖ MOTS-c    7 d    ⊕ MOTS-c
Recovery (full media)
⊖ MOTS-c    2 d    ⊕ MOTS-c

Rel. Crystal Violet (OD570)
***
Control    MOTS-c

**C** Energy Deficit Stress (Lipids Only)
⊖ MOTS-c    ⊕ MOTS-c
48 hrs

Rel. Crystal Violet (OD570)
***
Control    MOTS-c

**D**
Relative OCR
○ BSA
● Palmitate-BSA
***
Control    MOTS-c

**E**
MOTS-c-FITC    DAPI
0    0.5    4    24 (hrs)

**F**
PC2 (14%)
PC1 (16%)
△ Control    △ MOTS-c

**G**
Row Z-score
Control    MOTS-c

**H**
Heat Shock Responses
MOTS-c-related

**I** Pathways (GO)

NES
2
1
0
-1

FDR (-Log10)
● 1.25
● 1.50
● 1.75

Protein Regulation
- protein folding
- negative regulation of protein phosphorylation
- negative regulation of phosphorylation
- negative regulation of protein modification process
- negative regulation of transferase activity
- negative regulation of catalytic activity

Protein Metabolism
- positive regulation of protein catabolic process
- regulation of cellular protein catabolic process
- positive regulation of cellular catabolic process
- regulation of protein catabolic process
- positive regulation of catabolic process
- regulation of endopeptidase activity

Oxidative Stress
- response to oxidative stress
- cellular response to oxidative stress

Mitochondria
- mitochondrion organization

Cellular Metabolism
- cofactor metabolic process
- cofactor biosynthetic process
- small molecule biosynthetic process
- lipid biosynthetic process
- negative regulation of phosphorus metabolic process
- negative regulation of phosphate metabolic process

Cellular Death
- regulation of intrinsic apoptotic signaling pathway
- intrinsic apoptotic signaling pathway
- negative regulation of apoptotic signaling pathway
- negative regulation of neuron death
- regulation of apoptotic signaling pathway

Protein Transport
- establishment of protein localization to organelle
- nucleocytoplasmic transport
- nuclear transport
- protein localization to nucleus
- positive regulation of establishment of protein localization

Nucleic Acid Transport
- nucleic acid transport
- RNA transport
- establishment of RNA localization

Inflammatory Response
- regulation of cytokine production
- response to toxic substance

Misc. Cellular Response
- cellular response to hormone stimulus
- response to organic cyclic compound

Differentiation
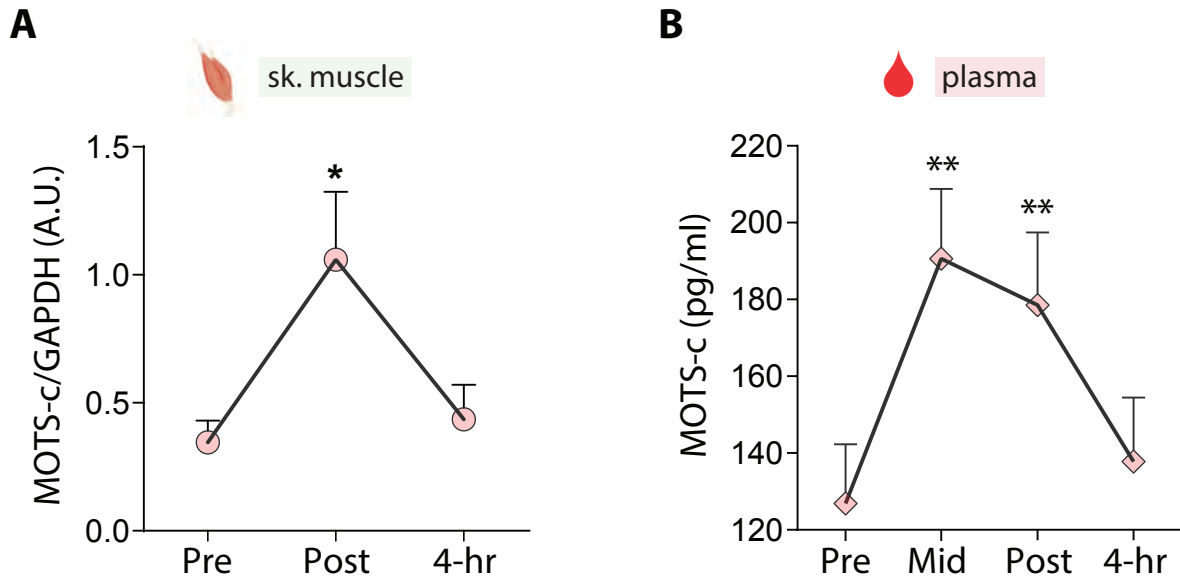- pattern specification process

**Fig. S1. MOTS-c levels in human muscle and plasma.** MOTS-c levels mea- sured by (A) Western blotting on human skeletal muscle collected pre-, post-exercise and 4- hours of resting and (B) ELISA on plasma from same individuals collected pre-, mid-, post- exercise and 4-hours of resting (n=10). Statistics by Wilcox-on matched-pairs signed rank test. **P<0.01
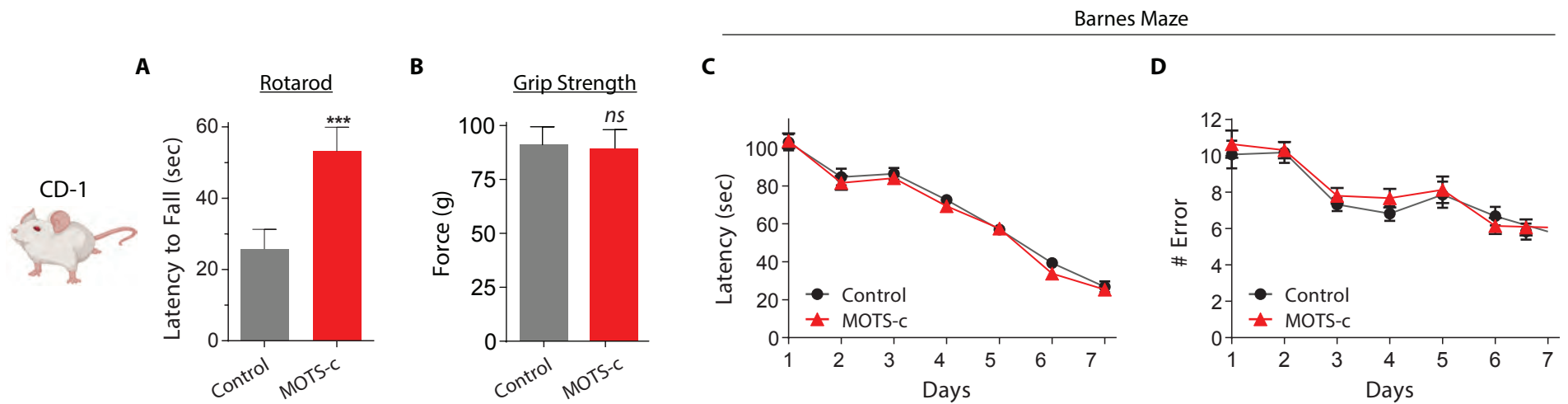
**Fig. S2. Rotarod, grip strength, and Barnes Maze tests in MOTS-c treated old mice.** (**A**) Summary of latency time to fall on the Rotarod test (n=15). The speed of the rotations increased from a starting speed of 24 rpm by 1 rpm every 10 seconds. (**B**) grip strength test. (**C,D**) Barned Maze performance in control and MOTS-c treated 12-week old CD-1 mice (n=15). (**C**) There was no changes in average time to find the escape box (latency) between control and MOTS-c treated mice. (**D**) There was no change in the number of errors made prior to discovering the escape box between groups. Errors were defined as nose-pokes or head deflections over false holes. Data expressed as mean +/- SEM of three 24-hour acquisition cycles. Student's t-test. *P<0.05, **P<0.01, ***P<0.001.
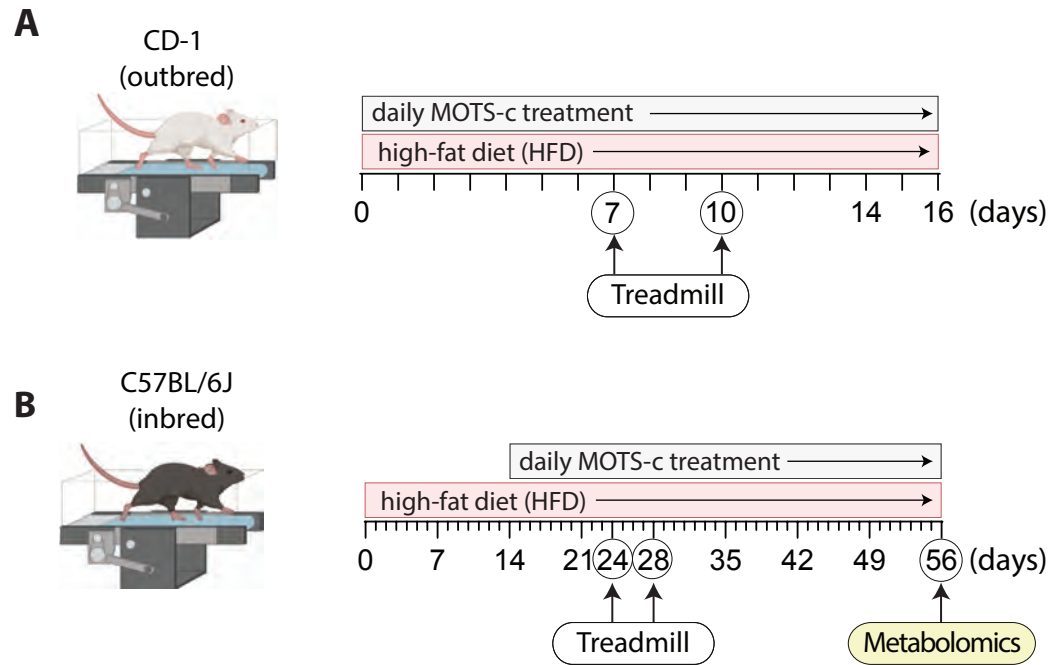
**Fig. S3. Outline of HFD mouse experiments.** Timeline of experiment for 12-week old male CD-1 (outbred) and C57BL/6J (inbred) mice fed a HFD or defined control diet. (**A**) CD-1 mice were fed a HFD and given daily intraperitoneal injections (IP) of MOTS-c (0, 5, or 15 mg/kg/day) from Day 0. Treadmill running tests were performed on Day 7 (fig. S4a) and Day 10 (Fig. 1e-h). Daily MOTS-c injections ceased at Day 16. (**B**) C57BL/6J mice were started on either a HFD or a defined control diet on Day 0 and continued uninterruptedly throughout the experiment. Daily MOTS-c treatment (15 mg/kg; IP) started on Day 14. Treadmill running tests were performed on Day 24 and Day 28 (10 days and 14 days after the start of MOTS-c treatment) (Fig. 1i-l; fig. S4b). Mice were treated daily until Day 56, at which time metabolomics was performed (Fig. 1m).
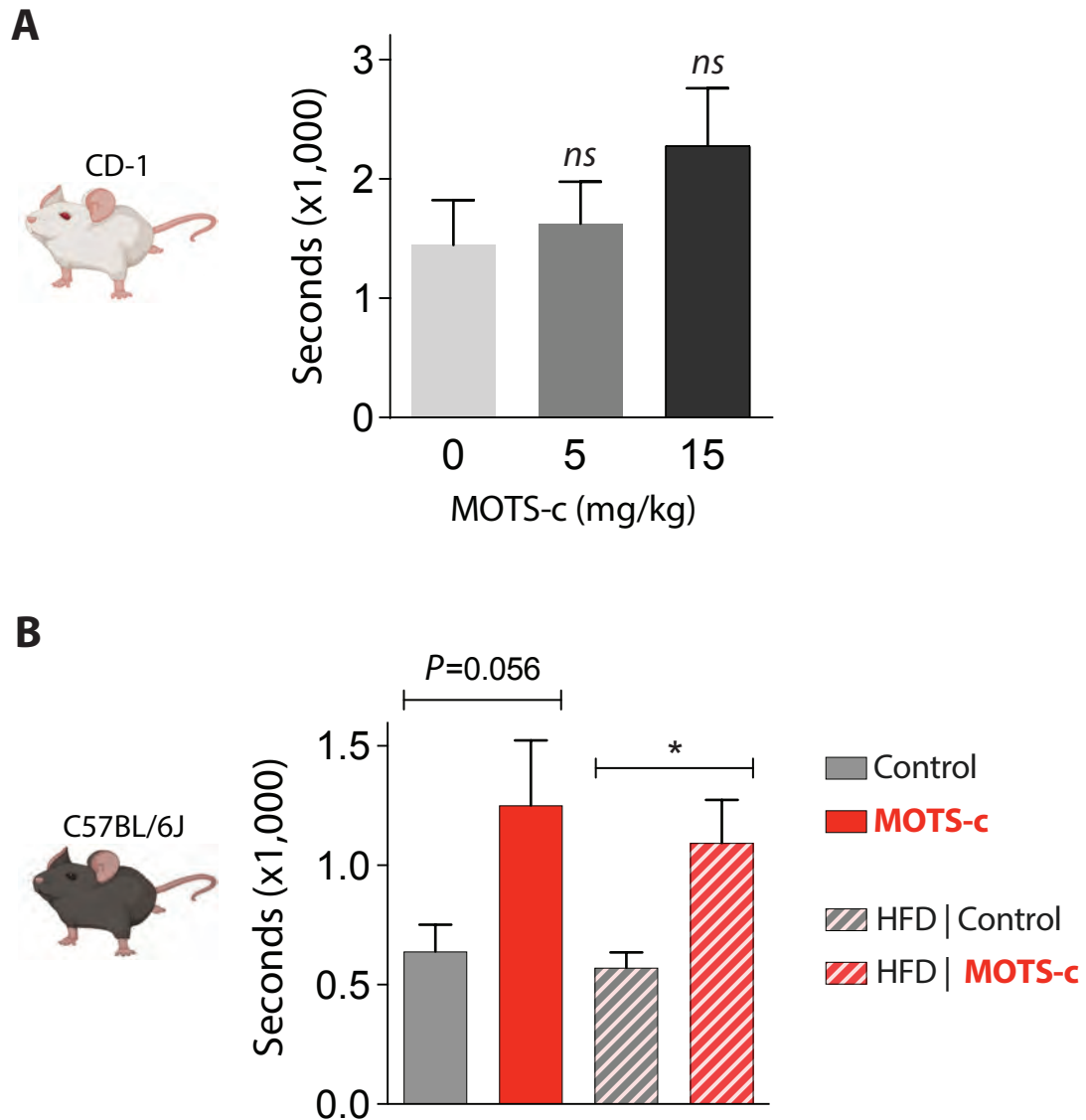
**Fig. S4. Initial running time of MOTS-c-treated young mice.** (**A**) Running time of CD-1 mice following seven days of MOTS-c treatment (n=5-6). MOTS-c (15 mg/kg/day) treatment showed a trend towards enhanced running performance. (**B**) Running time of HFD-fed C57BL/6J mice following 10 days of MOTS-c treatment (n=8). Data expressed as mean +/- SEM. Student's t-test. *P<0.05
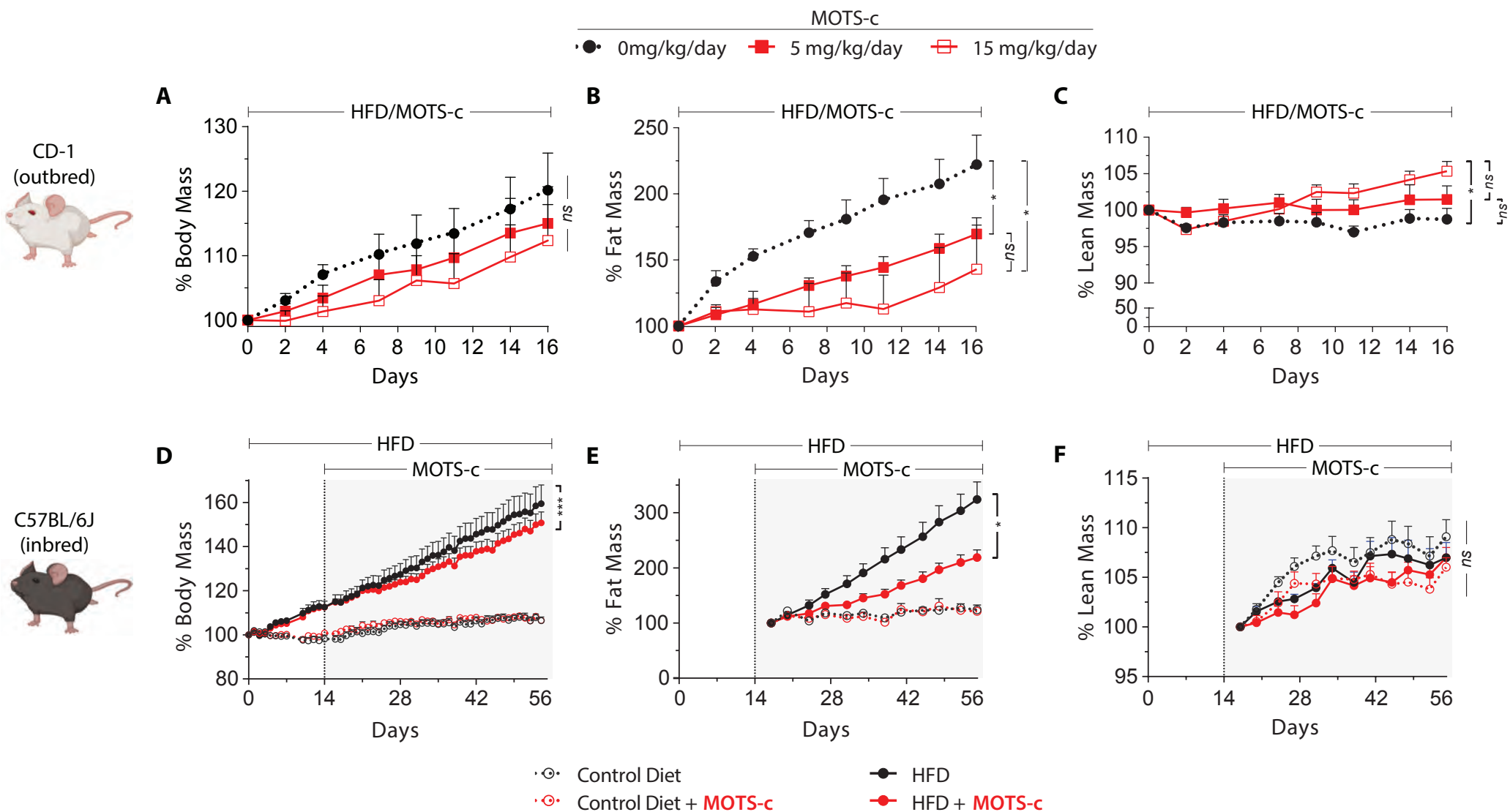
**Fig. S5. Body composition analysis on MOTS-c-treated young mice.** Body composition was measured non-invasively using a time-domain NMR analyzer. (**A-C**) Young CD-1 mice were treated daily with MOTS-c (0, 5, or 15 mg/kg/day;IP) for 16 days (n=5-6) and percent (**A**) body weight, (**B**) fat mass, and (**C**) lean muscle mass were measured. (**D-F**) C57BL/6J mice either on a HFD or a defined control diet and treated daily with MOTS-c (15 mg/kg/day; IP) or saline control (n=8) and percent (**D**) body weight, (**E**) fat mass, and (**F**) lean muscle mass were measured. The dotted line at Day 14 represents the start of MOTS-c treatment. Data expressed as mean +/- SEM. Significance determined by using two-way ANOVA (repeated measures). *P<0.05, **P<0.01, ***P<0.001.
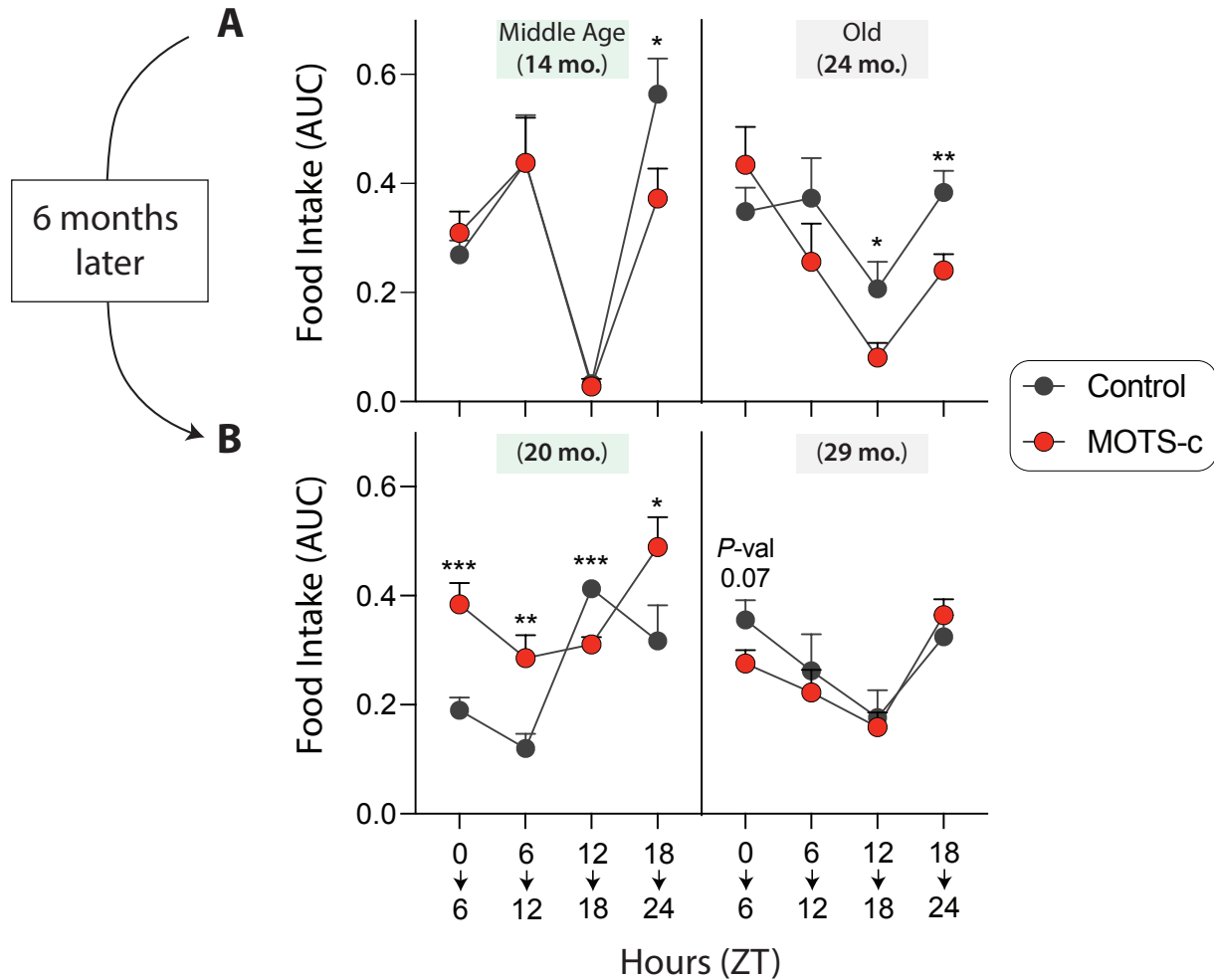
**Fig. S6. Circadian pattern of food intake in MOTS-c-treated old mice.** (**A**) The sum of continuous food intake measurements using metabolic cages divided into daily quartiles in MOTS-c-treated middle-age (14 months) and old (24 months) mice (n=4). (**B**) Measurements were taken 6 month later in same mice. Data expressed as mean +/- SEM. Student's t-test. *P<0.05, **P<0.01, ***P<0.001.
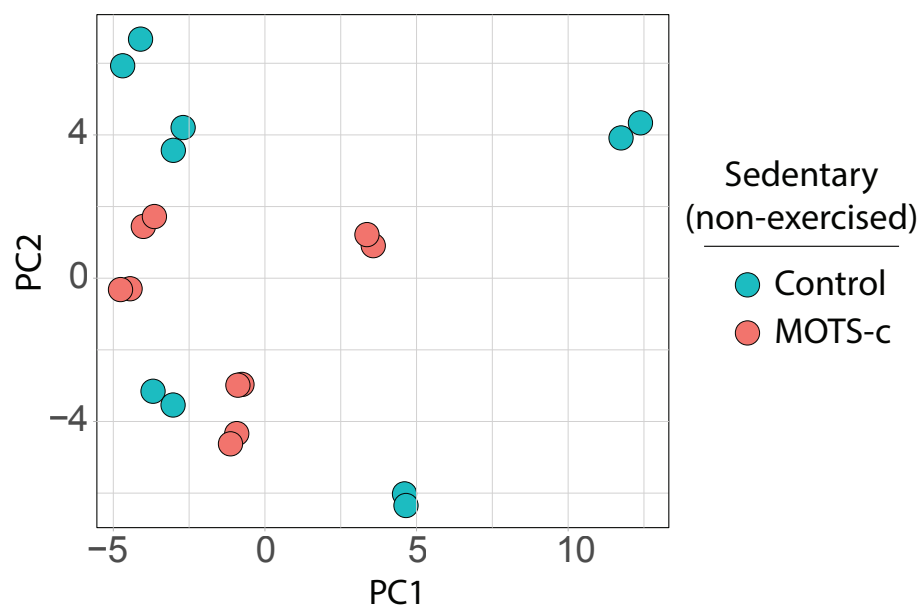
**Fig. S7. Metabolomic analysis on sedentary MOTS-c-treated old mice.** Skeletal muscle from sedentary (not treadmill-exercised) old mice (22.5 months) treated daily with MOTS-c (15 mg/kg/day) for 2 weeks (n=10) were subject to metabolomics and analyzed using PCA.
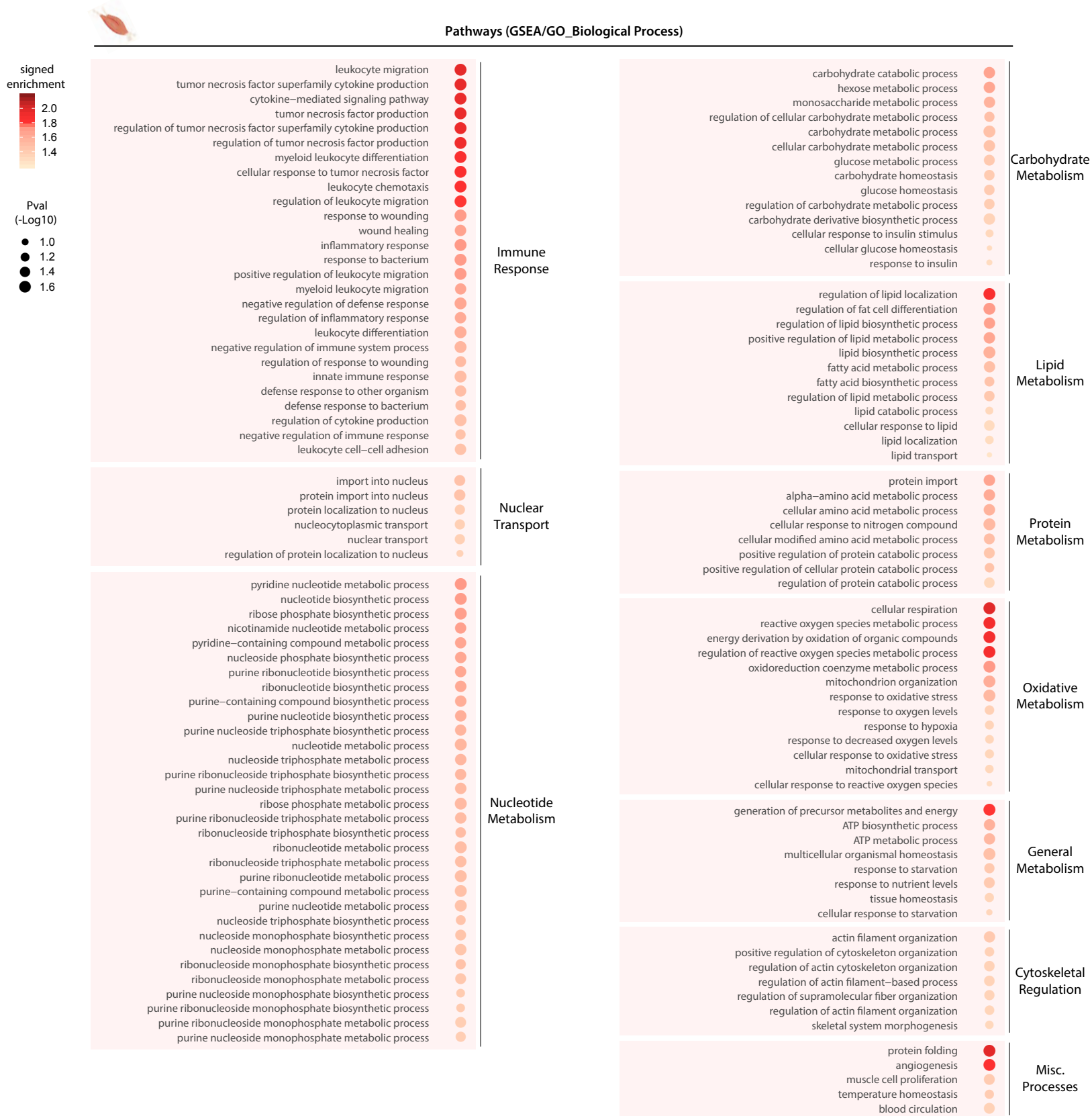
**Fig. S8. Gene expression analysis on skeletal muscle from exercised MOTS-c-treated old mice.** RNA-seq was performed on skeletal muscles from MOTS-c-treated old mice. Balloon plots of biological processes derived from Gene Set Enrichment Analysis (GSEA) using the Gene Ontology (Biological Process) database at a false discovery rate (FDR) < 15% (n=6).
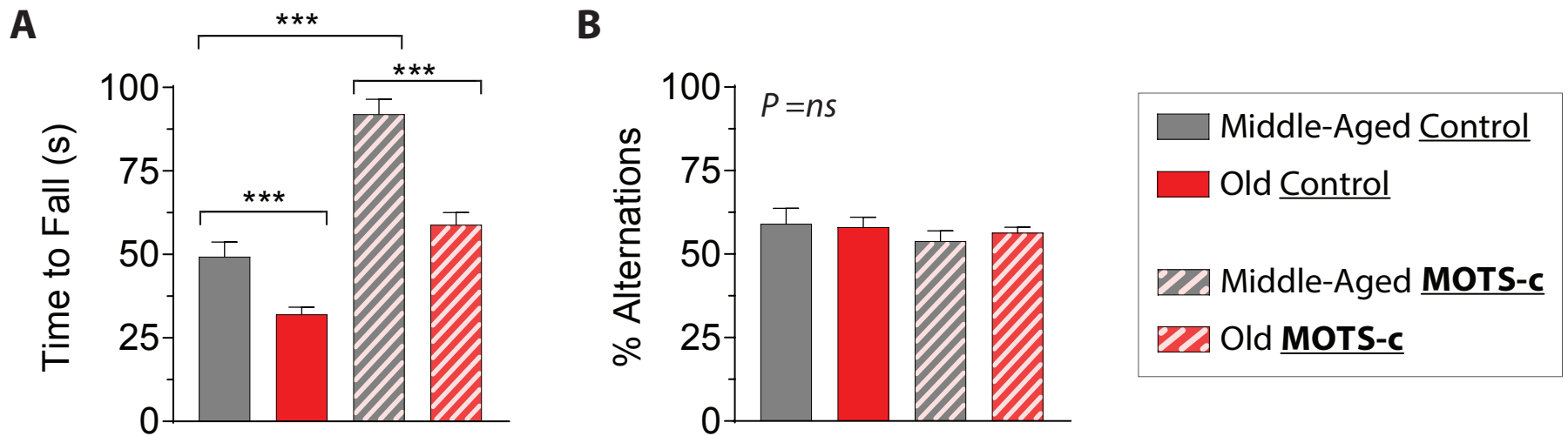
**A**

Time to Fall (s)

*** (bracket spanning Middle-Aged Control to Middle-Aged MOTS-c)

*** (bracket spanning Middle-Aged MOTS-c to Old MOTS-c)

*** (Middle-Aged Control vs Old Control)

**B**

% Alternations

*P =ns*

Middle-Aged <u>Control</u>
Old <u>Control</u>
Middle-Aged **MOTS-c**
Old **MOTS-c**

**Fig. S9. Rotarod and Y-Maze tests in MOTS-c-treated old mice.** Middle-aged (14 mo.; n=5-6) and old (24 mo.; n=17-19) mice were treated daily with MOTS-c (15 mg/kg/day; IP) and subject to (**A**) a rotarod test and (**B**) Y- maze test. Data expressed as mean +/- SEM. Student's t-test. ***P<0.001.
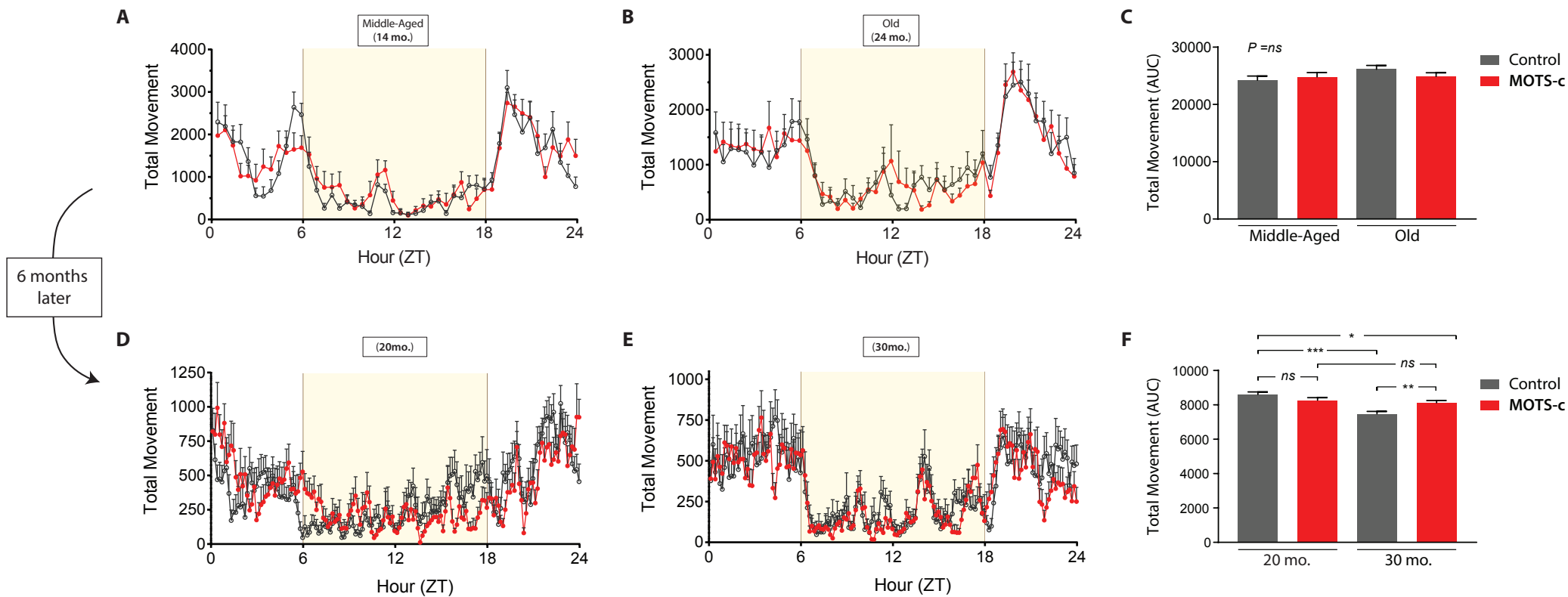
**Fig. S10. Total physical activity in MOTS-c-treated old mice.** Total movement [horizontal and vertical movement (XYZ-axis)] of MOTS-c-treated (**A**) middle-aged (14 mo.) and (**B**) old (24 mo.) mice were continuously measured using metabolic cages throughout the day for three days (n=4). (**C**) The sum of all measured movements is shown. (**D-F**) The procedure was repeated on the same mice after 6 months of LLII MOTS-c treatment. Data expressed as mean +/- SEM of three 24-hour acquisition cycles. Student's t-test. *P<0.05, **P<0.01, ***P<0.001.
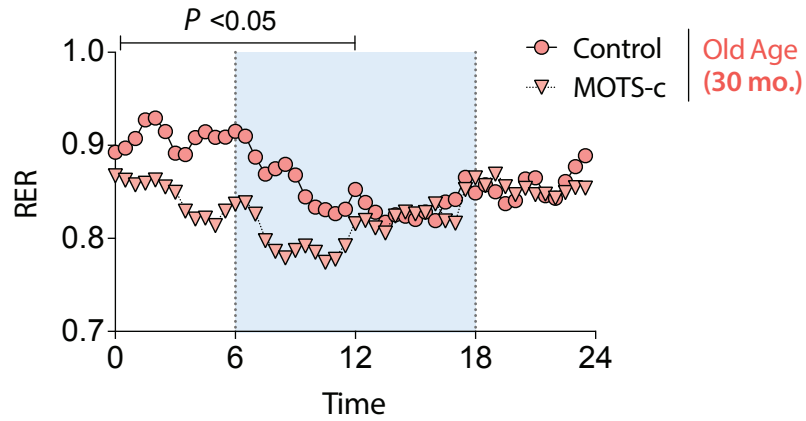
**Fig. S11. MOTS-c-dependent circadian fuel selection old mice.**
Respiratory Exchange Ratio (RER) measurements in LLII
MOTS-c-treated, or control, old mice (30 mo.; n=4). Shaded region
represents daytime (light cycle). Data expressed as mean +/- SEM of
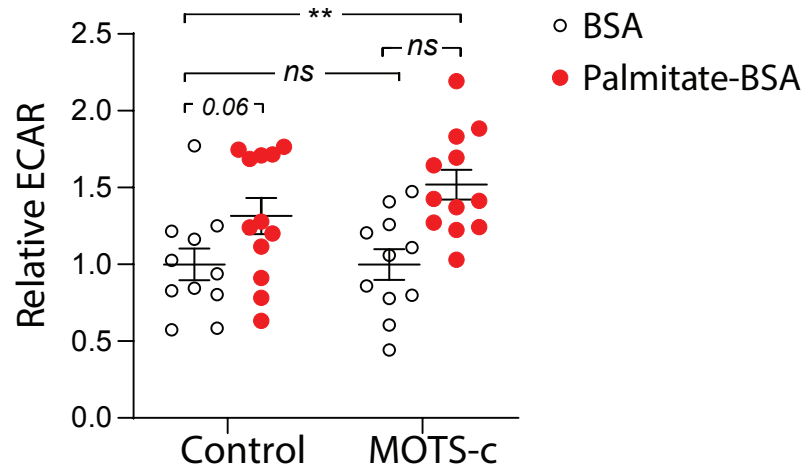three 24-hour acquisition cycles. Two-way ANOVA (repeated mea-
sures).

**Fig. S12. MOTS-c-dependent glycolytic rate in lipid-stimulated mouse myoblasts.** C2C12 mouse myoblasts were treated with MOTS-c (10μM) or saline control in nutrient- limited media (n=11-12). Real-time glycolytic flux determined by the extracellular acidification rate was measured using the XF96 Seahorse bioanalyzer. Prior to the start of the assay, nutrient-deprived cells were given either BSA alone or palmitate bound to BSA (palmitate-BSA) to determine the capacity to metabolize fatty acids. Data expressed as mean +/- SEM. Student's t-test. *P<0.05, **P<0.01, ***P<0.001.
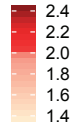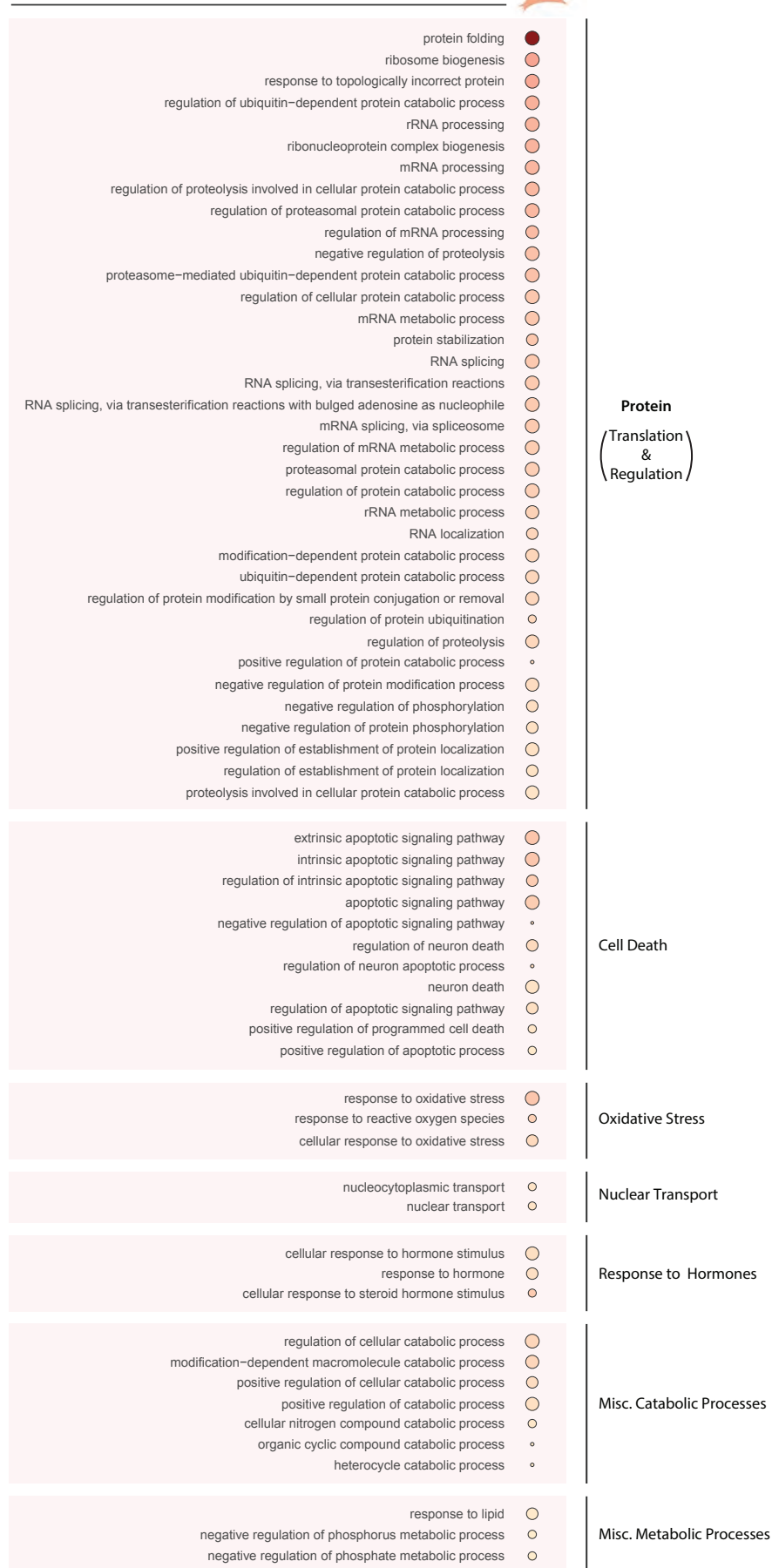
**Fig. S13. Gene expression analysis on MOTS-c-treated mouse myoblasts under metabolic stress.** RNA-seq was performed on C2C12 myoblasts following 48 hours of GR/SD with MOTS-c (10µM) treatment only once initially (n=6). Balloon plots of biological processes derived from Gene Set Enrichment Analysis (GSEA) using the Gene Ontology (Biological Process) database at a false discovery rate (FDR) < 15% (n=6).